Deformations on a Talings Dam Embankment Due to Its Heightening and Reservoir Filling

Sidnei Helder Cardoso Teixeira
Universidade Federal do Paraná: Universidade Federal do Parana
Paulo Roberto de Paiva
GHT Engenharia
Tennison Freire de Souza Junior
Universidade Federal do Rio Grande do Sul
Eduardo Conte
TechSolum Engenharia
Cezar Silva (cezarfalavigna@gmail.com)
Universidade Federal do Paraná: Universidade Federal do Parana https://orcid.org/0000-0001-7472-1431

Research Article

Keywords: Deformation, Displacements, Tailings Dam, Bidimensional numerical model, Tridimensional numerical modeling

Posted Date: May 17th, 2021

DOI: https://doi.org/10.21203/rs.3.rs-528290/v1

DEFORMATIONS ON A TALINGS DAM EMBANKMENT DUE TO ITS HEIGHTENING AND RESERVOIR FILLING.

Sidnei Helder Cardoso Teixeira.

PhD., Professor, Civil Construction Departament, Parana Federal University, Curitiba, PR, Brazil, E-mail: sidnteix@outlook.com. 0000-0002-3522-1706.

Paulo Roberto de Paiva.

Specialist, Director, GeoHydroTech (GHT), São Paulo, SP, Brazil, E-mail: ppaiva@ghtengenharia.com.br

Tennison Freire de Souza Jr.

Doctoral student, Civil Engineering Postgraduation Program, Rio Grande do Sul Federal University, Porto Alegre, SC, Brazil, E-mail: tennisongeotec@gmail.com. 0000-0003-0235-3152

Eduardo Conte.

Civil Engineer, Techsolum Engineering, Curitiba, PR, Brazil, E-mail: conte.eduardo@outlook.com.

Cezar Falavigna Silva [#].

Msc., Water Resources and Environmental Postgraduation Program, Parana Federal University, Curitiba, PR, Brazil. E-mail: cezarfalavigna@gmail.com. 0000-0001-7472-1431

[#] Corresponding Author

ABSTRACT – The purpose of this article is to evaluate the deformations of a compacted embankment dam, partially supported on tailings, through the use of two-dimensional and three-dimensional finite element models using PLAXIS® and TOCHNOG® software, respectively. The modeling was developed to simulate the construction of a complete dam stage, with a compacted embankment, a launched embankment platform, and the filling of the dam reservoir with the tailings. The material deformation parameters were calibrated so that the numerical modeling results are consistent with the data obtained from the instrumentation installed on the dam. The results made it possible to represent and understand the deformation mechanisms that occur during the construction of a raised stage and the filling of the reservoir.

Keywords – Deformation, Displacements, Tailings Dam, Bidimensional numerical model, Tridimensional numerical modeling.

Declarations

Funding: (Not applicable)

Conflicts of interest/Competing interests (There aren't any conflicting interests that could inappropriately bias their work)

Availability of data and material (Not applicable)

Code availability (Not applicable)

List of symbols

τ =
σ = Normal stress;
c = Cohesion intercept;
ϕ = Internal frictional angle;
σ_1 = Major main stress
σ_3 = Minor main stress
I_1, J_1, θ = stress invariants;
ε,ρ, θ = deviation stresses;
p', q = Stress paths parameters;
M = Parameter related to the angle of friction of the soil in triaxial compression;
γ = Specific weight;
E = elastic modulus.

1 – INTRODUCTION

Tailings dams are artificial embankment structures built from the accumulation of tailings from the ore beneficiation process. (Albuquerque, 2004; Azam e Li, 2010; Duarte,2008; Souza Junior, et al. 2018). Tailings dams are a particular type of dam built to store mill and waste tailings from mining activities. Currently, thousands of tailings dams worldwide contain billions of tonnes of waste material from mineral processing activity at mine sites. A number of particular characteristics make tailings dams more vulnerable to failure than water storage dams, such as: presence of embankments formed by locally derived fills (soil, coarse waste, overburden from mining operations and tailings); multi-stage raising of the dam to cope with the increase in solid material stored and effluent (plus runoff from precipitation) released; the lack of regulations on specific design criteria; dam stability requiring a continuous monitoring and control (Rico et al., 2008)

Nowadays, with the wide and intensive mineral extractive, more and more of this kind of dam are reaching the cubic million mark of storage and dozens of meters high, therefore, there has been some concerns about their behavior (Praça, 2019). The increase of compacted tailings confinement stress can generate the reduction of the friction angle due to the decrease of the post-peak shear resistance (Cavalcanti et al., 2003). With the Fundão/MG dam and Brumadinho/MG dam failures it has been created polices to the mischaracterization and decommissioning of the upstream tailing dams (Brazil, 2009). Until 2019, the registered mining dams with a reservoir superior to 50 hm^3 were 1,82% of the total of this kind of structure in Brazil, being most (61,02%) with a volume lower than 0,5 hm^3 (ANM, 2019). As for the height, from the registered dam's total, 20% don't have any information, 30% have height superior to 15 m and 50% are lower than 15 m (ANA, 2019).

With the embankment construction, the dam undergoes total and partial settlements. The stress versus soil deformation characteristics are extremally complex and the soil behavior is non-linear, inelastic, and highly dependent on the soil stress magnitude (Duncan, et al., 1980).

Azam and Li (2010) studied the failure events through time on mining tailings dams. Historically, the events occurred about 8 to 9 times in the 40s and 50s but reached a peak of 50 events during the 60s, 70s, and 80s. The elevation of the failure rate is due to the increase of the amount of these structures, due to the need for mineral extraction post World War II, because of the global demand for raw materials, minerals, and metals. In a survey accounting for 18401 local mines, the failure rate over the past 100 years is estimated to be at 1,2%. This is twice more the order of magnitude of accumulation dams' failures, which is about 0,01% according to ICOLD (2001) studies.

According to ANA (2019) data, from the registered dams in Brazil, about 21,00% have a high-risk category (CRI) and a high associated potential damage (DPA). The Risk Category (CRI) concerns aspects of the dam itself that may influence the likelihood of an accident: aspects of design, structure integrity, state of conservation, operation and maintenance and compliance with the Safety Plan. The Potential Associated Damage (DPA) is the damage that can occur due to rupture, leakage, soil infiltration or malfunction of a dam, regardless of its probability of occurrence. It is graded according to the loss of human life and social, economic impacts and environmental.

As for tailings dams (ANM, 2019), there are 436 registered in Brazil, of which 60,09% present high DPA, and 11,24% have a high CRI. The nature of the involved risks and the possible impacts due to a dam breach suggests that the control and monitoring of these structures should be done carefully so preventive or corrective measures are implemented promptly.

According to Chrzannowski e Massiéra (2004), the study of stress versus deformation behavior on dams are very important, once this knowledge allows to predict possible problems, such as the appearing of transversal cracks, longitudinal fissures, arching effects and stress concentration, hydraulic fracturing, development of yield zones and instrumentation damage, besides allowing to minimize the effects of these problems.

This article has the purpose of presenting the assessment of the stress versus deformation behavior of a mining tailings dam with the use of two-dimensional and three-dimensional finite

element models. For this, the complete construction of one of the dam's stages – stage 13 – was evaluated so that it was possible to understand the factors that occasioned the rotation and displacement movements.

2 – STUDY DATA

The studied dam forms a reservoir to store mining tailings. The structure acts as the last environmental control point for the effluents that flow to a small stream basin. The dam foundation is predominantly constituted by metamorphically rock outcrops with a low degree of weathering, called phyllite, fine rock grains, basically composed of quartz and sericite, and characterized by the presence of a penetrative parallel plane foliation. The phyllite was semi-weathered, with multiple colors, predominating purplish and grayish tones.

The foliation is affected by folding, which conditions the spatial disposition of foliation. It was detected two folding systems, the first and main one has NE-SW direction axes and an SW low angle dip that is for upstream of the dam. This system is predominant on the right embankment and central portion of the dam. The second system has an NW-SE direction and an NNW low angle dip and is predominant in the left embankment.

The valley, where the dam is implemented, is an open kind with smooth abutments, set up by a floodplain of a stream in its central part. The dam crest is at El. 648,00 m after the construction of stage 13.

The dam landfill is homogeneous in a compacted embankment, done with a reddish colluvium clay and clayey-silt soil. The dam had until then, 13 heightening stages, and had 77 meters height and a length of 4890 meters. The downstream slope has an inclination of 1V:2H, 3 meters wide berms every 6 meters, and the upstream slope is continuous with a 1V:1,8H inclination.

The dam's first eight heightening stages were built with the downstream method, in which the heightening is built with the increase of the dam landfill towards downstream from the previous stage. After the 8th stage, based on observations of the good behavior of a landfill dam posted over the tailing's reservoir, has also been used the upstream method. For this method, a compacted embankment was built over a landfill platform posted on the tailings, alternately with the downstream method, in such a way that the dam axis remained, approximately, in the same position, resulting in what was called a modified centerline method.

The advantages of this method consist of the maintenance of the flux produce from the mineral processing. In addition to safeguarding the technical criteria for the stability of the structure, as the tailings are discharged on the upstream method compacted landfill region, concomitant, it was built the downstream method compacted embankment. This reduced the construction time for the dike and allows the industrial processes to remain continuous or suffer minimal interferences on the mineral tailings discharge.

In each stage is heightened not only the compacted embankment but also the upstream landfill platform, in addition to raising (filling) the tailings reservoir. The landfill is a material platform created between the tailings and the compacted landfill and has the function of stiffening the base where will be done the dike construction activities, that is, it facilitates the earthwork. Besides this, it consists of a stable support transition layer, once it is supported by the tailings deposited in the reservoir and acts as a partial foundation of the compacted embankment, consequently minimizes the settlement in the heightening region.

In this study, it was assessed the deformations on the dam that are caused by its heightening. On the two-dimensional analyses, it was evaluated the stage 13 heightening, while the three-dimensional analyses assessed the stage 12A and 13, concomitantly. Figure 1 presents the display of theses heightening:

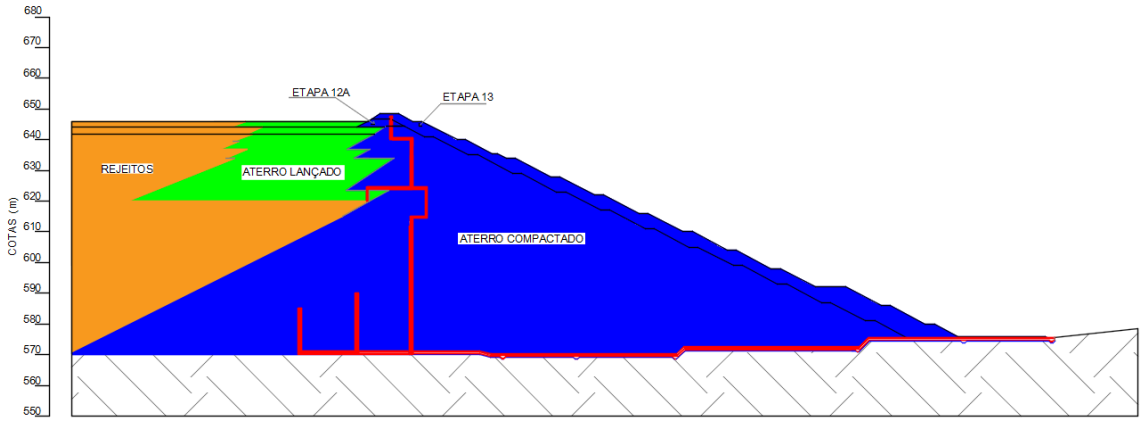

Figure 1. Dam typical section – stages 12A and 13

2.1 – Instrumentation evaluated

The model calibration was done using the data provided by the dam's instrumentation system. to assess the vertical displacement, it was considered the readings of settlement plates MR-1A, MR-1C, MR-2A, MR-2C, MR3A, and MR 3C. For the horizontal displacements, it was evaluated inclinometers I-1, I-2, and I-3 readings.

2.2 – Mohr-Coulomb Yield Criteria

The Mohr-Coulomb model was chosen because of the frictional material and its simplicity (Chen and Han, 1988; Wood, 2004). The Mohr-Coulomb yield criterion represents a generalization of the Tresca criteria and describes materials with frictional nature (Schager, 1998). According to Lambe and Whitman (1969), in the Mohr-Coulomb criteria, Mohr circles represent the material stress state, and the maximum stress points are tangent by stress curves, which the rupture only occurs when the soil shear stress surpasses the shear stress resistance. In other words, the Mohr circles relate the normal stress (σ) and the shear stress (τ)

Coulomb (1776) cites that the soil shear resistance would be controlled by the cohesion intercept and friction angle portion, in which the normal stress variation enables the increment or reduction of the resistive capacity, following the equation (1) and figure 2a.

$$\tau = c + \sigma \tan \phi \tag{1}$$

Where:
σ: Normal stress;
c: Cohesion intercept;
ϕ: Internal frictional angle.

The resistance function expression in terms of principal stresses is presented in equation (2):

$$\frac{\sigma_1 - \sigma_3}{2} = \frac{\sigma_1 + \sigma_3}{2} \sin \phi + c \cos \phi \tag{2}$$

Chen and Han (1987) demonstrated the construction of the tridimensional yield surface in terms of stress invariants (I_1, J_1, θ) and deviation stresses (ε,ρ, θ) of the Mohr-Coulomb criteria. Equation (3) and (4) present theses formulations based on Figure 2b illustration:

$$\int(I_{1,}J_2,\theta) = \frac{1}{3}I_1\,\sin\phi + \sqrt{J_2}\sin\left(\theta+\frac{\pi}{3}\right)+\frac{\sqrt{J_2}}{\sqrt{3}}\cos\left(\theta+\frac{\pi}{3}\right)\sin\phi - c\cos\phi = 0 \qquad (3)$$

$$\int(\varepsilon\rho,\theta) = \sqrt{2}\sin\phi + \sqrt{3}\rho\sin\left(\theta+\frac{\pi}{3}\right) + \rho\cos\left(\theta+\frac{\pi}{3}\right)\sin\phi - \sqrt{6}c\cos\phi = 0 \qquad (4)$$

In which $0 \le \theta \le 60°$, so that if $\theta = 0°$ (traction meridian) and $\theta = 60°$ (compression meridian).

In the Mohr-Coulomb criteria, the failure stress under compression is greater than under traction. The yield surface is represented by a hexagonal base pyramid (offset between vertices of 60°) irregular in the main stress space (Nadai π plane), the cross-section being an octagonal polygon, illustrated in figure 2b. In the Mohr-Coulomb model, exposed by Potts and Zdravkovi (1999), sharp corners are observed when tracing the function in the octahedral space of the main tensions (see figure 2b)

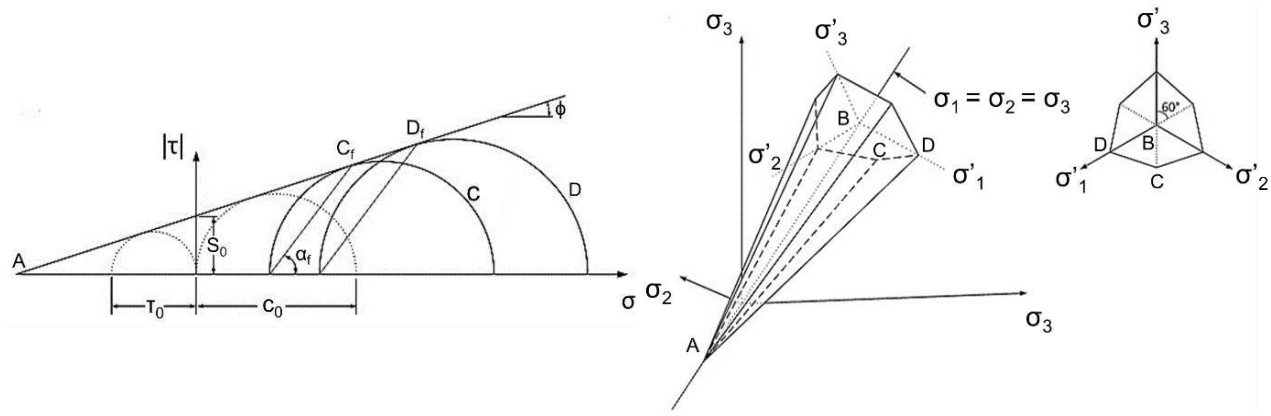

(a) **(b)**

Figure 2. Mohr-Coulomb Criteria: a) Rupture envelope; b) Failure surface. (Source: Labuz and Zang, 2012)

Huallanca (2004) cites that the Mohr-Coulomb yield criteria applied to a perfect elastoplastic model have a null yield function. The perfect elastoplastic model has a fixed yield surface and defined by resistive parameters and axial (σ_1) and confining (σ_3) stresses, according to figure 3, based on equations (2), (3) and (4)

For the dam stress versus deformation analyses, it was used the Mohr-Coulomb yield criteria with a linear elastic perfectly plastic model (see figure 3a), which behavior is characterized elastic until yield stress or yield limit (σ_o) subsequently undergoing purely plastic deformations from the constant maintenance of the same σo, as described in Fernandes (2011). According to Chen and Han (1988), in this model the stiffening effect is negligible, being the plastic deformation triggered by the constant stress flow. The authors affirmed that the yield surface of the perfectly plastic material is maintained unaltered, being observed the generalized formulation in equation (5). Figure 3b illustrates the limit (yield surface) between the elastic and plastic zones.

$$f(\sigma_{ij}) = F(\sigma_{ij}) - K \qquad (5)$$

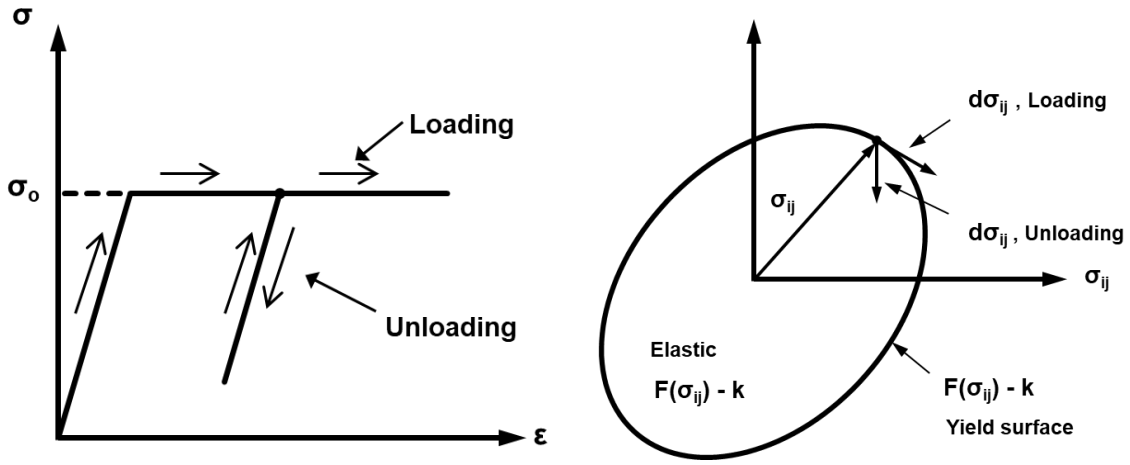

(a) **(b)**

Figure 3. Elastic perfectly plastic model: a) Stress vs deformation behavior; b) Loading and unloading yield surface (Cheb e Han, 1988).

Equation (6) describes in terms of flow surface (Wood, 2004)

$$f(\sigma) = f(p,q) = q - Mp' \tag{6}$$

Which the M value – Equation (7):

$$M = 6\frac{\sin\phi}{3 - \sin\phi} \tag{7}$$

Where:
p',q: Stress paths parameters;
M: Parameter related to the angle of friction of the soil in triaxial compression.

2.3 – Numerical modelling calibration and validation

The deformability parameters used in the bidimensional and tridimensional analyses are present um table 1. The values are the result of an iterative calibration process of the numerical model, through bidimensional analysis, using the software PLAXIS®.

Table 1 – Adopted geotechnical parameters due to the calibration

Soil	γ (kN/m³)	c' (kPa)	ϕ' (°)	E (kPa)	μ
Foundation	10 (sub)	200	24	160.000	0,35
Compacted landfill	19 (nat)	10	30	25.000	0,30
Saturated compacted landfill	10 (sub)	33	26	20.000	0,33
Dumped landfill	19 (nat)	10	31	15.000	0,35
Saturated dumped landfill	9 (sub)	10	31	10.000	0,37
Filter	18 (nat)	0	33	50.000	0,35
Saturated filter	8 (sub)	0	33	50.000	0,35
Tailings	7 (sub)	0	12	2.000	0,40

The adopted parameters are from the drained conditions, once all the deformations on the dam occur slowly for this study analyses. It was used the natural specific weight for the soils above the phreatic surface and the submerged weight for the soils below it. Besides, it was adopted a cohesion intercept equal to 10 kPa for the compacted landfill to minimally represent the soil apparent cohesion.

In the calibration process, initially, the values for the elasticity modulus and the Poisson coefficient were adopted from the ranges of values suggested by Bardet (1997) database. After this, the calibration and validation of the deformability parameters of the elastic model (Young's modulus and Poisson coefficient) were done by the comparison of the vertical and horizontal displacements calculated by the model and the data from the settlement plates and inclinometers. The parameters values were, through the many simulations done, being altered until the behavior of the model was similar to the one observed on the dam through the instrumentation results. The calibration process is iterative and needs the modeler's sensibility to adjust the parameters until the behavior is similar to the real one observed on the dam. The procedure is summarized below.

Regarding calibration of the vertical displacement data, the readings of six settlement plates were considered: MR-1A; MR-1C; MR-2A; MR-2C; MR-3A and MR 3C. These plates were installed on the launched landfill platform since the previous stages (8 and 8a) construction. The plates with the "A" denomination are located according to the "A" alignment, at a distance of 19.5 m upstream of the dam reference line of stage 13, and the plates ending in "C" are installed according to the "C" alignment, at 39.5 m upstream of this same line. For the calibration, simulations were done considering the construction of the dam starting from stage 8 to stage 13, allowing the comparison between the results of the numerical model and the settlement plate readings. Table 2 presents the real settlement values registered by the field plates from the installation to the end of the construction of stage 13.

Table 2. Accumulated settlements of Stage 8 until the end of stage 13 construction

Plate	Settlement (m)	Plate	Settlement (m)
MR-1A	2,16	MR-1C	2,11
MR-2A	1,96	MR-2C	2,02
MR-3A	1,97	MR-3C	3,16
Average	**2,03**	***Average***	**2,43**

The numerical simulation results indicated that, in the position of the plates installed along the alignment "A", the accumulated settlements were about 2.0 m, the plates installed along the alignment "C", the settlement were about 2.5 m. So, it is noticed that the values measured by the plates and the numerical model have a very good fit. The discrepancies between the real and simulated values are less than 10 cm, which is considered a very good fit, considering the height of the dam and the thickness of the embankment and tailings masses.

Additionally, it was compared the accumulated settlements during the construction of stages 12A and 13. The model results indicated that, for the plates along the "A" alignment, the accumulated settlements were 0.43 m, and for the plates along the "C" alignment, the settlements were 0.40 m. Table 3 presents the settlement values registered by the plates during the construction period of stages 12A and stage 13. Again, the calculated and observed values are very close, with differences below 10 cm.

Table 3. Accumulated settlements during the constructive periods of stages 12A and 13

Plate	Settlement (m)	Plate	Settlement (m)
MR-1A	0,33	MR-1C	0,52
MR-2A	0,30	MR-2C	0,41
MR-3A	0,52	MR-3C	0,60

Plate	Settlement (m)	Plate	Settlement (m)
Average	**0,38**	***Average***	**0,51**

Regarding the calibration of the horizontal displacements, it was based on the readings of three inclinometers I-1, I-2, and I-3, installed at the highest section of the dam, and they served as a comparison base to the values obtained through the numerical simulations. Due to the short period recorded (January to August of 2005), the direct comparison of the calculated and measured values is restricted, however, it is possible to use the readings to compare the magnitude order of these values. This way, in this evaluation, it is considered only stage 13 construction. Figure 4 illustrates the horizontal displacements profiles along the depths, obtained by the numerical model, for the stage 13 construction simulation, in the positions where the inclinometers are installed. It is noticed that the maximum displacements for all the inclinometers are of the order of 55 mm downstream.

According to the instrumentation reading, done during the seven months of construction of stage 13, the maximum observed horizontal displacements were 28 mm and 33.1 mm for inclinometers I-1 and I-2, respectively, towards downstream. For inclinometer I-3, it was observed a downstream maximum displacement of 54 mm, but this inclinometer presented different results from the other because it is installed in a depth of about 30 meters below the bedrock top. The I-3 inclinometer data indicated that the foundation of the dam is moving significantly downstream, a fact that is not noticed by the other instruments of the dam. Considering the restricted period of readings, it is possible to affirm that exists compatibility between the magnitude order of the recorded and simulated values. However, a more adequate comparison between the inclinometer data and the simulation results will only be possible when there is a minimum period of reading of the inclinometers of two consecutive years. This is because the constructive planning of the dam always considers the simultaneous construction of two stages, one for upstream and one for downstream. The downstream construction stage takes two years to be completed.

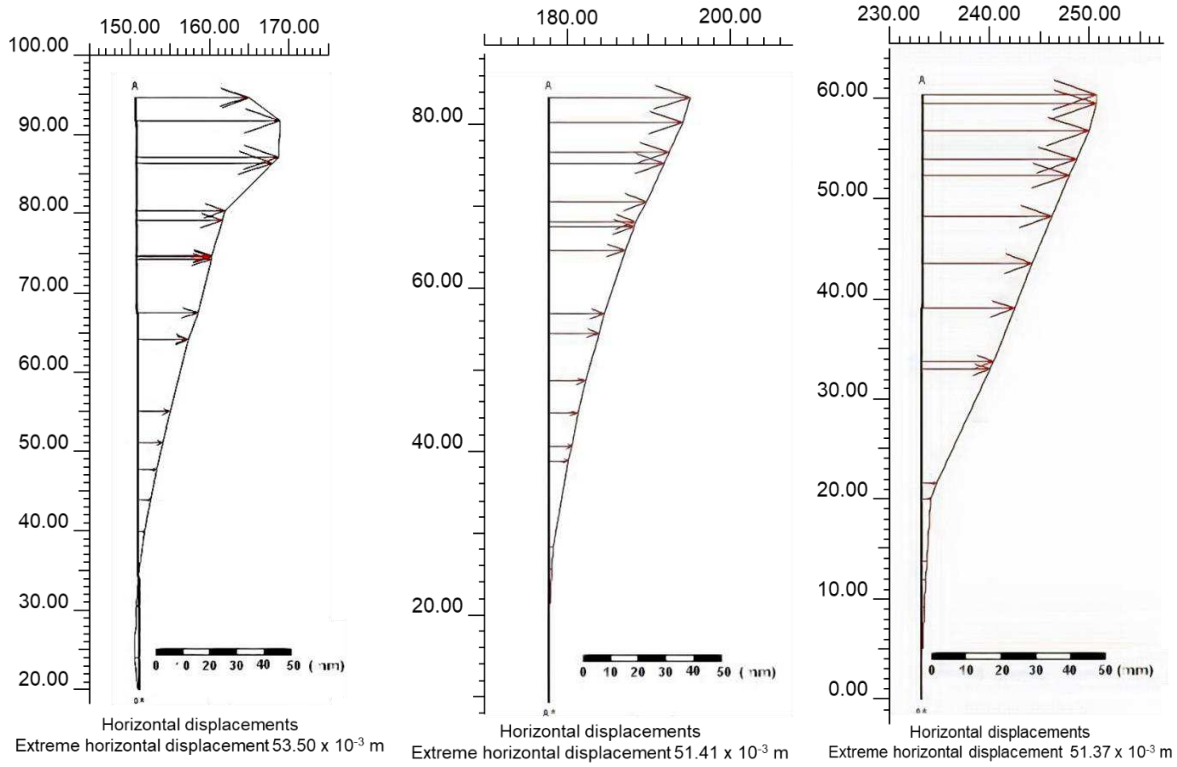

Figure 4. Numerical model horizontal displacements results for the inclinometers (x Direction)

Finally, it appears that calibration methods such as the present one, based on the comparison of numerical model data with instrumentation records, appear in geotechnical studies such as those by

Shahba and Soltani (2016). These authors carried out an assessment of stress versus strain in the Taham earth dam and compared the two-dimensional analyzes (Geostudio® and FLAC®) with three-dimensional (PLAXIS®), obtaining data regarding horizontal strains, vertical strains, and stresses similar to the values obtained dam instrumentation

3 – BIDIMENSIONAL STRESS VERSUS DEFORMATIONS ANALYSES

The bidimensional analyses were done using the PLAXIS® software, having two objectives: calibrate the deformation geotechnical parameters to be used on the tridimensional analyses (as described before); perform a qualitative and quantitative assessment of the dam's behavior during heightening stage construction.

3.1 – Method

The numerical model development was done through the staged construction of the dam. This procedure is important and should be applied to geotechnical structures with a compacted embankment, once the construction of such structures is not done instantly and the soil's stress history has effects on the results and behavior of the model. This way, it was developed preliminary stages simulating the construction until stage 12.

Next, was developed stage 13, the main objective of this study, in which it was pretended to analyze the structural behavior during its construction. This stage was modeled in the phases, provided for in the executive sequencing in the field:

a) Construction of the compacted embankment;
b) Construction of the upstream casted landfill platform;
c) Reservoir filling.

The results had the objective to evaluate the construction effect of a heightening stage over the existing dam embankment, through the horizontal and vertical displacements and volumetric deformations. It was assessed separately the effects caused by each of the three phases and it was also evaluated the global effect generated by the overlay of the three phases, that is, by the end of the heightening of the dam (compacted landfill and launched landfill platforms) and the reservoir filling. The appraised section is located in the center of the valley, in which the tailings layer deposited in the reservoir have a greater thickness, and, consequently, the dam has the biggest height.

3.2 – Results

3.2.1 – Phase 1: Compacted embankment construction

In this stage, it was assessed the deformation behavior of the existing dam when the heightening embankment is built. The dam was heightened by the modified centerline method, as described before. The stage 13 compacted landfill is partially supported by the already built compacted embankment (downstream) and partially by the launched landfill platform (upstream). The vertical displacements (see figure 5a) have a greater magnitude on the crest due to the proximity of the more deformable materials, such as the tailings and cast landfill, that are upstream, being the maximum value around 21 cm. These displacements reduce along with the depth. On the downstream slope surface, the place most far of the deformable materials, the maximum vertical displacements were about 14 cm.

As the horizontal displacements (see figure 5b) they were directed downstream along the downstream dam slope, in a place close to the top of the filter, with values around 5.5 cm. However, on the tailings and launched fill, the displacements were upstream, with a maximum value of about

8.5 cm. In a general manner, upstream of the filter, the displacements were directed to upstream, while downstream of the filter, there is a movement towards downstream, this indicates that there is a horizontal dislocation of these two parts, with expansion horizontal deformations.

This way, it is possible to observe that when the compacted landfill part is being heightened, there is an indication of the occurrence of a rotational movement of the dam crest (with upstream sinking), due to the proximity of deformable materials, like tailings and launched fill.

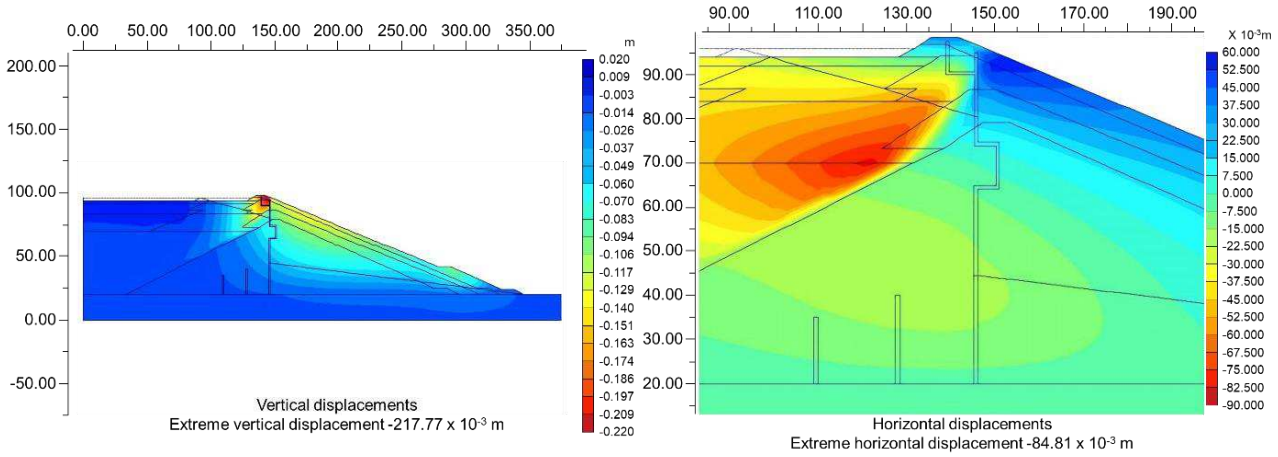

(a) **(b)**

Figure 5. Dam displacements caused by the stage 13 compacted embankment construction: a) vertical (m); b) horizontal (x 10^3 m).

Assessing the volumetric deformations (figure 6), it is noticed that on the major part of the dam embankment there are compression deformations with low magnitudes, around 0,3%. Only a small region located over the filter the volume variation was positive, indicating that on the spot occurred the soil expansion. The maximum deformation value was 4,7%. The soil expansion is believed to be related to the rotational movement of the dam crest which incurs in the horizontal expansion deformations in this region, and, consequently, positive volumetric deformations (expansion).

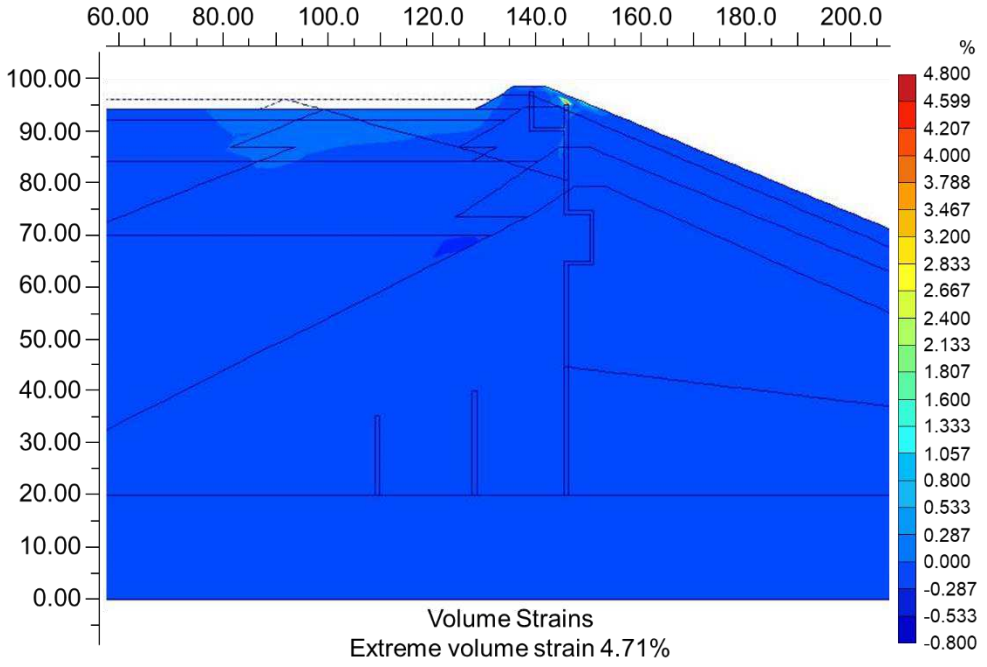

Figure 6. Volumetric deformations on the dam caused by the construction of the compacted embankment of stage 13.

3.2.2 – Phase 2: Construction of the upstream launched landfill platform

In phase 2, it was evaluated the deformations behavior on the existing dam when built the upstream launched landfill platform, and after the construction of the previous phase (compacted embankment). Stage 13 launched fill platform is partially supported by the tailings and partially supported by the compacted embankment, built previously. The vertical displacements (figura 7a) were more pronounced, especially under the launched fill, have greater magnitude on the surfaces, and present maximum values around 22 cm. The casted landfill construction promoted a small lift of the tailings surface located upstream, with maximum values at 5 cm. As the impact on the already built compacted embankment, it was observed that the vertical displacements are greater upstream of the dam crest (approximately 12 cm) compared to the downstream (around 8 cm).

The horizontal displacements (see figure 7b) on the launched landfill and tailing occurred towards upstream and reached maximum values around 13 cm on the tailings. The displacements provoked by the compacted embankment were, in general, to downstream, with maximum values around 2 cm inside the dam mass. However, near the crest, the displacements were towards upstream, with values around 9 cm

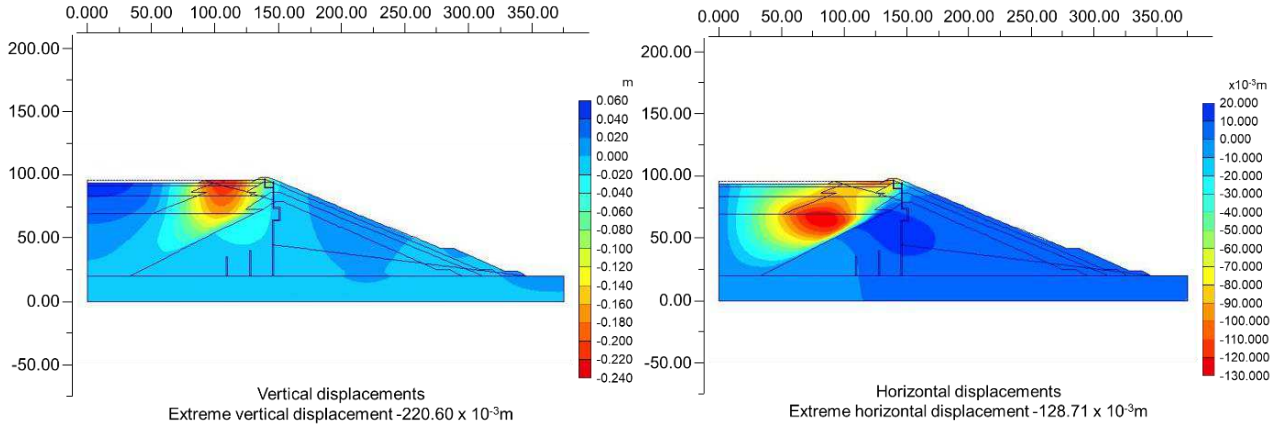

(a) **(b)**

Figure 7. Vertical displacements on the dam, caused by the construction of the stage 13 launched fill: a) Vertical; b) Horizontal.

The compression volumetric deformation (figure 8) was of low magnitude and occurred mainly on the tailings, under the launched landfill, and, on a lower scale, on the own casted landfill, with maximum values around 0,7%. On the other hand, on the dam crest, it was possible to see expansion volumetric deformations, with values up to 1,6%, which, again, are the result of the dam crest rotation with sinking to upstream, behavior also noticed during the launched fill platform construction.

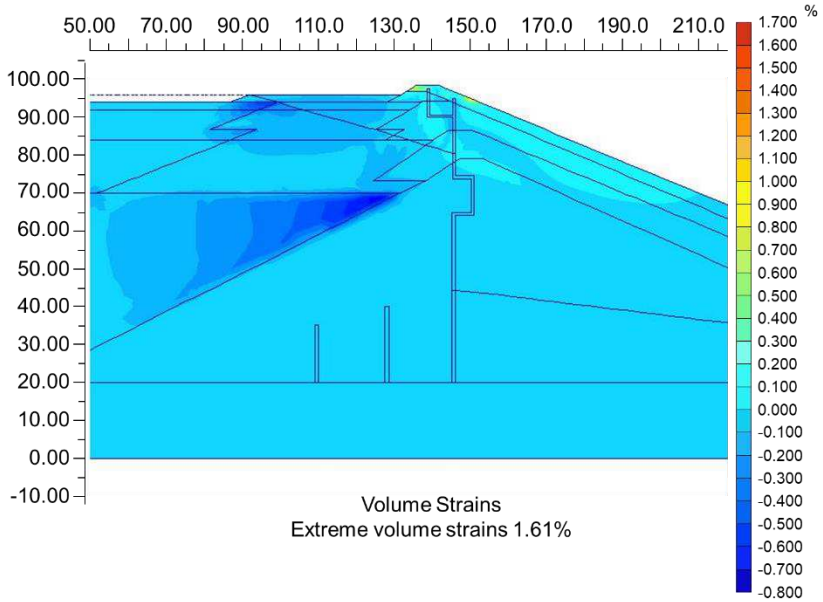

Figure 8. Volumetric deformations on the dam caused by the stage 13 launched landfill construction.

3.2.3 – Phase 3: Filing

In phase 3, it was assessed the dam deformations due to the filling of a new layer of tailings in the reservoir, after the heightening of the compacted soil and launched landfill. The vertical displacements (see figure 9a) occurred almost exclusively on the tailings, with maximum values around 28 cm near the surface. The upstream end of the launched landfill platform was also affected by the filling of the reservoir suffering vertical displacements with values around 12 cm. As the crest of the dam approaches, the vertical displacements approach zero, which is indicative of the rotation of the launched landfill.

The horizontal displacements on the landfills (see figure 9b) launched and compacted, due to the reservoir filling, resulted directed exclusively towards downstream. The major displacements were on the tailings under the launched landfill, with maximum values around 5 cm.

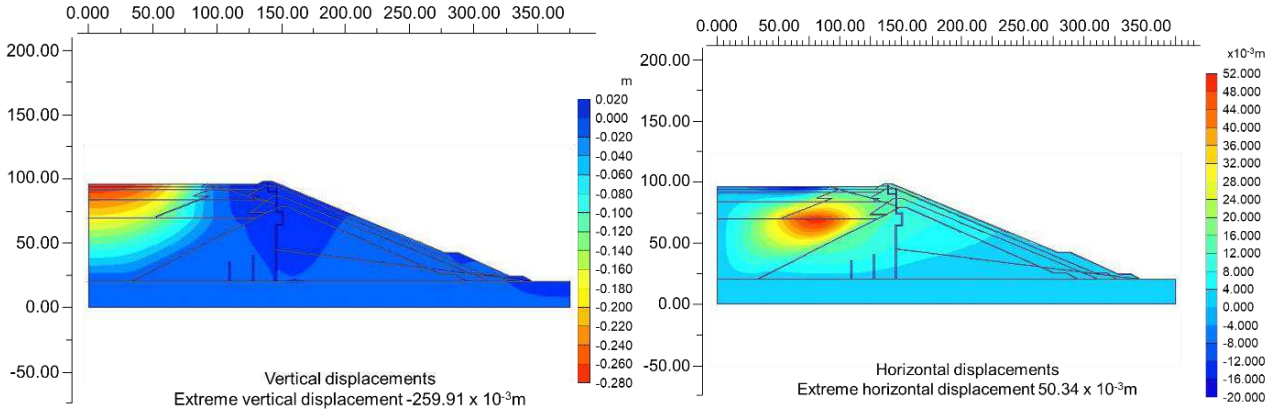

(a) **(b)**

Figure 9. Vertical displacements on the dam originated by the stage 13 reservoir filling: a) Vertical; b) Horizontal

The volumetric deformations (figure 10) occurred mainly on the tailings and were compression ones, with average values of low magnitude, about 0,3%. However, on the launched landfill surface there were expansion volumetric deformation, with values around, 0,2%, and these seem to be

related to the flexion suffered by the launched landfill massif since one end is over the tailings (more deformable material) and the other end is near the stiffer material (compacted embankment).

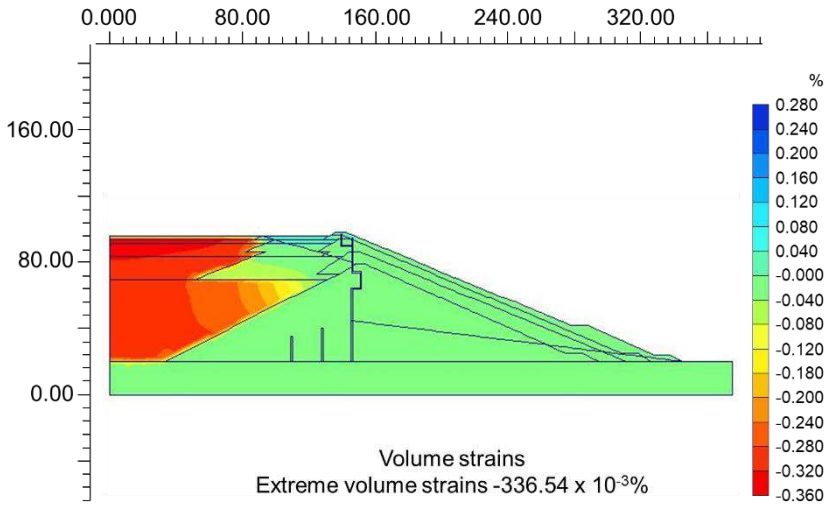

Figure 10. Volumetric deformations on the dam caused by the stage 13 tailings reservoir filling

3.2.4 – Global effect

Finally, deformations that occurred on the existing dam after the heightening on the dam and filling of the reservoir were evaluated, considering the overlay of effects referred to the end of the dam heightening and reservoir filling.

The resulting vertical displacements (see figure 11a) were more pronounced at the crest of the dam and on the surface of the launched landfill platform, with maximum values around 30 cm. The Vertical displacements decrease with depth and as it dislocates downstream. Therefore, there is a sinking of the upstream section of the dam in relation to the downstream section.

The horizontal displacements of the compacted embankment (see figure 11b) were towards downstream and more pronounced closer to the slope surface, with maximum values around 5 cm. The horizontal displacements on the launched landfill and tailings presented under the launched landfill were upstream, with maximum values of about 13 cm. In general lines, it can be said that upstream of the filter, the horizontal displacements occurred towards upstream, and downstream of the filter, the displacements were towards downstream.

The volumetric deformations of the tailings (see figure 12a), under the casted landfill, occurred with low magnitude, around 1,2% on the maximum and they were compression ones. The deformations over the filter, near the crest of the dam, were expansion ones with significative magnitude, reaching about 5%. On the most part of the massif, the volumetric deformations were small. The sinking of the tailings, launched landfill and the dam's crest compared to the rest of the compacted embankment, promotes something similar to flexion on the dam, generating expansion deformations on the crest. For this reason, the volumetric deformations in this region are expansion ones.

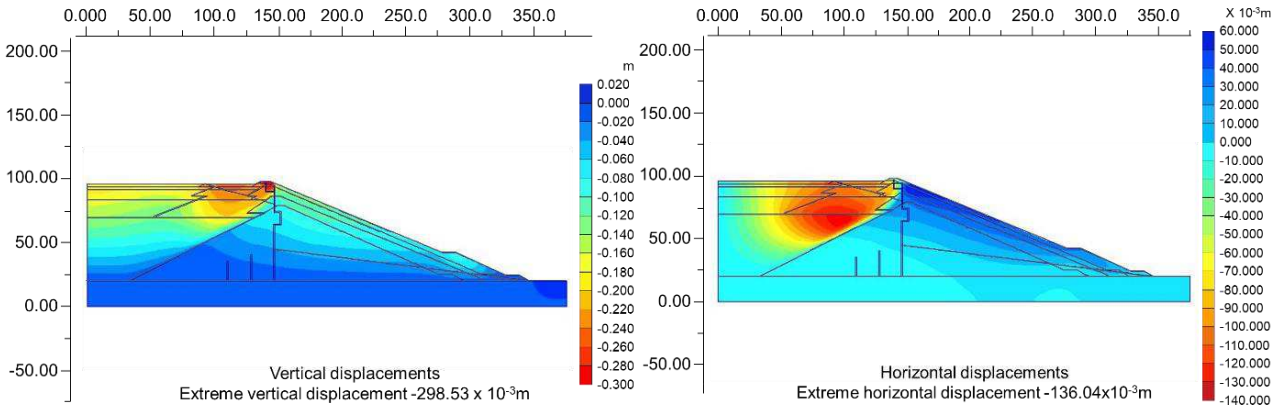

(a) **(b)**

Figure 11. Displacements on the dam due to the stage 13 construction and filling of the reservoir: a) Vertical; b) Horizontal

At this stage, it was also evaluated the yield occurrence (see figure 12b), through the Mohr-Coulomb yield criteria, as cited previously. The main sites for soil yield were on the vertical filter, close to the crest of the dam, and on the slope of the launched landfill. The yield occurred by tension at some points and by compression at other points, usually located below the points where the yield took place by traction. On the upstream slope of the launched landfill, the yield is related to the pronounced displacements that occurred due to the proximity of the most deformable material. The yield of the soil close to the crest happens by tension. This behavior pattern is in line with the thesis that a phenomenon similar to bending is occurring on the highest elevations of the dam due to the rotation of the upstream material (more deformable) in relation to the downstream portion of the compacted embankment (stiffer).

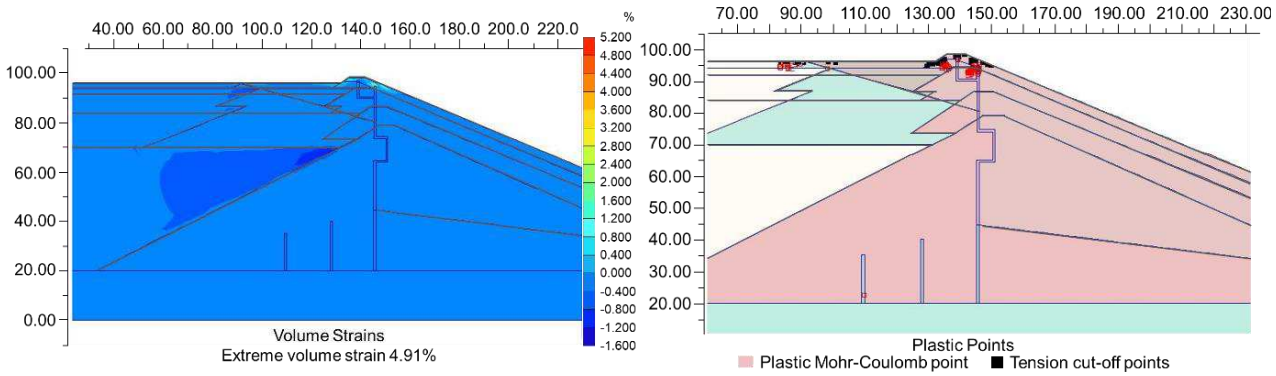

(a) **(b)**

Figure 12. Yield on the dam caused by stage 13 construction and reservoir filling: a) volumetric deformations; b) Evaluation of yield concentration points of the dam

4 – 3D STRESS-DEFORMATION ANALYSES

The tridimensional analyses were done using TOCHNOG, V. 2004 software. This tool uses the finite element method and has constitutive models and applications designed for the modeling of the geotechnical structure.

4.1 – Method

For the tridimensional numerical modeling, it was used tetrahedral finite elements with 4 nodes. The geotechnical parameters values were calibrated using the bidimensional analyses, done previously, and present in table 1.

The modeling of irregular tridimensional structures, such as the case study dam, has additional complicated factors when compared to bidimensional analyses, especially regarding the definition of finite elements in space and changes in their properties over time during simulations. In this way, some simplifying hypotheses were adopted to enable the modeling of the structure, minimizing the number of finite elements and processing time. The main simplifying hypotheses were:

a) Simplification of the dam geometry;
b) Disregarding the presence of filters;
c) Use of submerged specific weight for the soils below the phreatic level.

The tridimensional model (figure 13) was built with the purpose to assess the construction effect of two heightening stages over the existing embankment. These stages are 12A and 13. In a preliminary stage, it was built the whole existing massif, before the heightening. Nest I was built in a single stage the heightening corresponding to stages 12A and 13, with the simultaneous construction of the compacted embankment, launched fill platform, and reservoir filling. In this way, it was evaluated the global effects of the heightening and reservoir filling over the existing embankment, referring to stages 12A and 13.

Figure 13. Finite elements of the surface of the model

The evaluated parameters were the vertical and horizontal displacements, the volumetric deformations, and the areas where plasticization occurs the yield.

4.2 – Results

The horizontal displacements of the transversal direction to the dam axis (see the bidimensional section, figure 14a) were evaluated both on the surface of the soil and inside the massif. On the soil surface, the horizontal displacements were toward downstream, on the region downstream of the axis, and on the region upstream of the axis, the horizontal displacements were toward upstream. The maximum values were 4.2 cm towards upstream and 15.5 cm towards downstream. The behavior indicates a tendency for the two parts to move away from each other, as already observed in two-dimensional analyzes

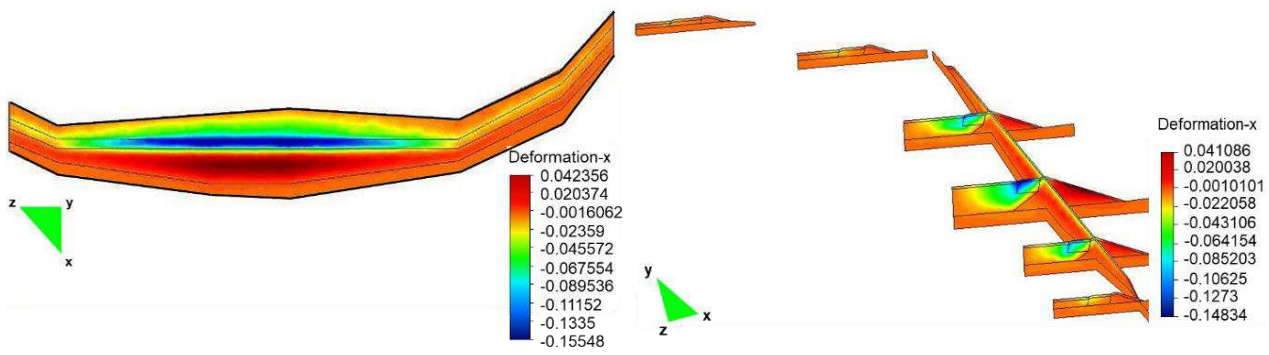

(a) **(b)**

Figure 14. Horizontal displacement on the x direction: a) soil surface; b) massif interior (values in meters)

Horizontal displacements were also evaluated in the longitudinal direction to the dam axis in two regions: soil surface and embankment interior. On the soil surface (figure 15a), it was noticed that the tailings, launched fill, and compacted embankment displacements were always from the abutment to the center of the valley. On the center of the valley, it is found the highest tailings thickness and where the dam is the highest. The opposite occurs on the abutments. The maximum displacements were around 2.5 cm. On the central part of the dam (figure 15b), almost the isn't longitudinal displacements. In the massif interior, it is also observed that the horizontal displacements were towards the center of the valley and larger as they approach the surface, reaching values around 2.5 cm.

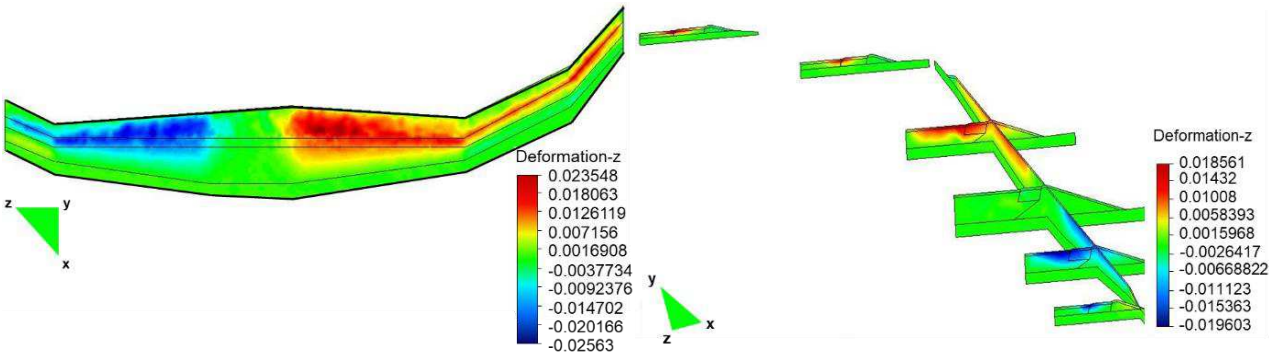

(a) **(b)**

Figure 15. Horizontal displacements on the z direction: a) on the soil surface; b) on the massif interior (values in meters)

The vertical displacements were more pronounced on the tailing and the launched fill, in the sections located on the center of the valley, reaching values up to 50 cm on the soil surface. However, these displacements occur on the whole extension of the dam. On the surface (figure 16a), the highest values were observed on the launched fill slope and get smaller as approaches the dam's crest. This indicates a rotation of the launched fill, as observed on the bidimensional analyses. In the interior of the embankment (figure 16b), on the base of the launched fill, it turns out that vertical displacements are more pronounced as they move away from the dam's centerline, with values between 15 cm and 40 cm on the highest sections, again confirming the rotation of the launched fill. The vertical displacements decrease as they approach the abutments, also indicating the rotation around the transversal direction, showing greater vertical displacements on the center of the valley and smaller displacements of further places. Along the centerline, inside the massif, it was also found that the displacements were more pronounced in the center of the valley.

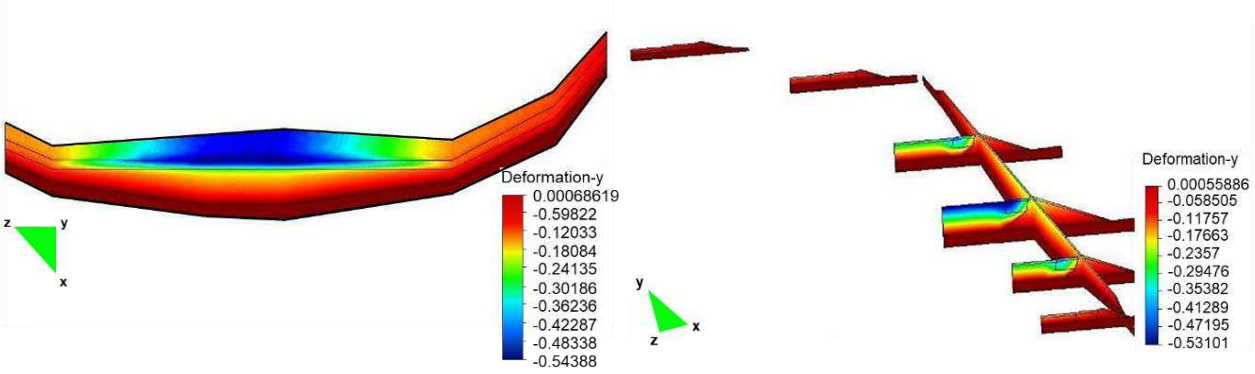

(a) **(b)**

Figure 16. Vertical displacements on the embankment: a) soil surface; b) in the interior of the massif (values in meters)

In the terms of volumetric deformations, on the transversal direction (figure 17a), it is observed that there is expansion deformation along the dam axis, with values around 0.4%, on the surfaces of the soil, and compression along the slope toe of the launched fill, with values around 0.3%. On the longitudinal direction along the axis (figure 17b), the deformations were very small and more intense closer to the abutments. It should be warned that in these regions the axis of the dam is no longer aligned with the longitudinal direction as in the straight section, making the analysis more complex. On the central straight section, it can be noticed that the deformations wavered between null and the compression ones, and on the side of the central section, between null and expansion. The behavior is similar to a fixed ended beam (on the end of the straight section, close to the abutments), where the deformations in the upper fibers were characteristic of expansion variation, close to the fixed end, and compression, in the central region.

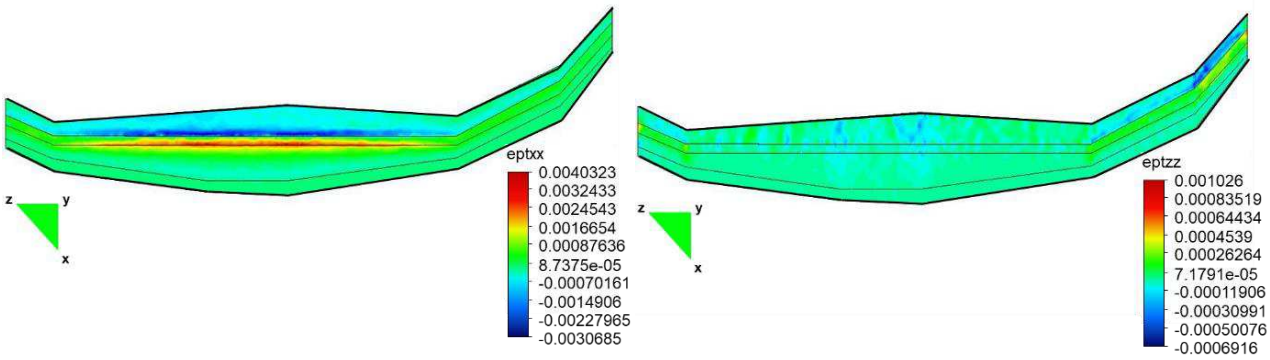

(a) **(b)**

Figure 17. Total deformations of: a) soil surface on the x direction; b) soil surface on the z direction (values in m/m)

Areas of occurrence of soil plasticization were also evaluated. On the transversal direction (see figure 18b), on the surface, the soil suffered yield along the dam axis due to the occurrence of expansive deformations, as said before. Evaluating the same parameter on the longitudinal direction (Figure 18b), it was noticed the presence of considerable small expansion yield deformations, at the end of the dam axis, when it is closer to the abutments.

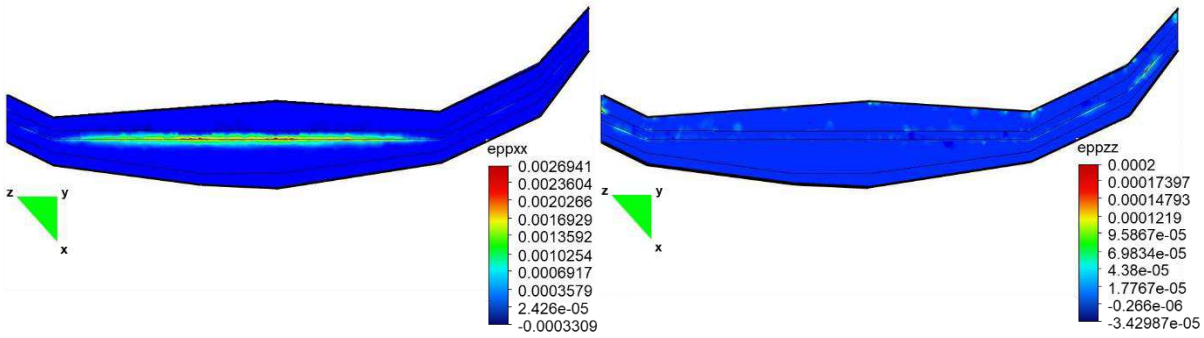

(a) **(b)**

Figure 18. Yield deformations: a) soil surface on the x direction; b) soil surface on the z direction (values in m/m)

In summary, after the assessment of the obtained results, It was possible to notice that the stress versus deformation behavior by the numerical model shows a significant coherence with the field behavior, once the answer of the numerical model is suitable to the observed physical phenomena, they being the occurrence of yield zones in places where already shown cracks and consonance of the calculated displacements values through data instrumentation.

5 – FINAL CONSIDERATIONS

Based on the presented comments it is possible to establish, regarding the bidimensional analyses, that:

a) The elastic parameters and methodology used on the stress versus deformations analyses led to results compatible with readings of the dam instrumentation;
b) The soil of the dam massif is subject to plasticization. The region near the dam crest, where tensile stresses occur, would be subject to the eventual appearance of superficial longitudinal cracks;
c) The difference between vertical displacements of the compacted embankment surface and launched fill, during the construction stages, would be the mechanism that would favor the superficial soil yield. The launched fill surface suffers bigger vertical displacements than the soil on the crest of the dam. That can generate something similar to a bend, with expansion deformations of the surface and compressive ones on the interior of the dam;
d) During the construction of the compacted embankment, depending on the installation position of the inclinometers, upstream displacements can be registered;
e) The construction of the launched fill and the reservoir filling cause only small magnitude downstream displacements on the soil downstream of the vertical filter;
f) In the launched landfill, the displacements are upstream when the compacted embankment and the launched landfill are built, and, downstream, when the reservoir is filled with tailings.

Based on the tridimensional analyses, it is possible to make the following comments:

a) Although it was adopted some simplifying hypothesis on the tridimensional modeling of the dam, the obtained results are coherent, because the allowed to clarify some field observed phenomena;
b) The yield deformations on the top of the downstream slope are expressive and are in line with what was observed in the field;
c) The fact that there is a thick tailings layer under the launched landfill favors the occurrence of plasticization on the compacted embankment, near the crest, once the tailings elastic (Young's) modulus is very inferior to the other materials modulus. The cohesion and friction

developed along the contact between the compacted embankment and launched landfill transfer the referred rotation movement to the dam massif;

d) The analysis results indicate that the tailings' vertical movement is more intense in the center of the valley, decreasing in the direction of the abutment. This movement is related to the thickness of the deposited tailings layer;

e) It was verified a small magnitude movement in the longitudinal movement of the dam, from the abutments to the center. This movement is mainly attributed to the tailing height variation along the dam, as well as the variation of the tailings layer height under the launched landfill. On the central part of the dam, where the height of the tailings is practically constant, there aren't displacements in the longitudinal direction;

f) The normal deformations in the longitudinal direction have a small expression. The yield deformations in this direction are minimum and well distributed along the dam axis, however, they are almost gone on the central part of the dam. These deformations must be associated with the tailings' height variation under the launched landfill on the longitudinal direction of the dam.

6 – ACKNOWLEDGMENT

The authors would like to thank CAPES (*Coordenação de Aperfeiçoamento de Pessoal de Nível Superior*) for promoting research at the PPGECC (*Programa de Pós-Graduação de Engenharia de Construção Civil*) at the Federal University of Paraná.

7 – REFERENCES

Albuquerque LH (2004) Evaluation of the geotechnical behavior of iron ore tailings dams through of piezocone tests. Dissertation, Ouro Preto Federal University [in Portuguese] http://www.repositorio.ufop.br/handle/123456789/6145

ANM (2019) Public Mining Dams Integrated System (SIGBM). https://app.anm.gov.br/sigbm/publico. [in Portuguese]. Accessed 31 October 2020

ANA (2019) Dam Safety Report. http://www.snisb.gov.br/portal/snisb/relatorio-anual-de-seguranca-de-barragem/2019 [in Portuguese]. Accessed 31 October 2020

Azam S, Li Q (2010) Tailings Dam Failures: A Review of the Last One Hundred Years. Waste Geotechnics: 50-53. https://ksmproject.com/wp-content/uploads/2017/08/Tailings-Dam-Failures-Last-100-years-Azam2010.pdf

Bardet JP (1997) Experimental Soil Mechanics. Prentice Hall, New Jersey

Brazil (2019) Resolution 13 (August 8th, 2019). Establish regulatory measures aimed at ensuring the stability of mining dams, notably those built or raised by the method called "upstream" or by the method declared as unknown and provides other measures. Diário Oficial da República Federativa do Brasil, Brasília, 2019. [in Portuguese]

Cavalcante ALB, Hernandez AP, Assis AP (2003) Extension of the angle of friction-tension-density relationship of Bolton (1986) to granular tailings of iron ore. In: Procedings of 5º Congresso Brasileiro de Geotecnia Ambiental, Porto Alegre [in Portuguese].

645 Chen WF, Han DJ (1988) Plasticity for Structural Engineers. Springer-Verlag, New York

646 Chrzannowski AS, Massiéra M (2004) Modelling of deformations during construction of large earth
647 dam in the La Grande Complex, Canada. Technical Sciences 7:109-121.
648 http://www.uwm.edu.pl/wnt/technicalsc/ts7_2004/10_7_2004.pdf

649 Coulomb CA (1776) Essai sur une application des regles des maximis et minimis a quelquels
650 problemes de statique relatifs a la architecture. Academie Royale Des Science 7:343–387

651 Duarte AP (2008) Classification of mining tailings and industrial waste dams in the state of Minas
652 Gerais in relation to risk potential. Dissertation, Minas Gerais State Federal University [in
653 Portuguese]. http://hdl.handle.net/1843/BUDB-8AUPNJ

654 Duncan JM, Byrne P, Wong KS, Mabry P (1980) Strength, stress-strain, and bulk modulus
655 parameters for finite element analyses of stress and movements is soil masses. Report No.
656 UCB/GT/80-01, University of California, College of Engineering, Berkeley, California

657 Huallanca REZ (2004) Failure mechanisms in high open mining slopes. Dissertation, University of
658 São Paulo [in Portuguese]. https://doi.org/10.11606/D.18.2004.tde-21092007-161107

659 ICOLD (2001) Tailings dams risk of dangerous occurrences: Lessons learnt from practical
660 experiences. Bulletin 121

661 Lambe WT, Whitman RV (1969) Soil Mechanics. John Wiley & Sons, New York

662 Praça LP (2019) Chemical and mechanical behavior of zinc mining tailings under low to high
663 effective stresses. Dissertation, Rio Grande do Sul State Federal University [in Portuguese]
664 http://hdl.handle.net/10183/199181

665 Fernandes MM (2011) Soil Mechanics: Concepts and fundamental principles [in Portuguese].
666 FEUP, São Paulo

667 Potts DM, Zdravkovic L (1990) Finite element analysis in geotechnical engineering. Thomas
668 Telford, London

669 Rico M, Benito G, Díez-Herrero A (2008) Floods from tailings dam failures. Journal of Hazardous
670 Materials 154(3):79-87. https://doi.org/10.1016/j.jhazmat.2007.09.110

671 Schager GS (1987) Mohr-Coulomb Failure Criterion Expressed in Terms of Stress Invariants.
672 Journal of Applied Mechanics 65:1066-1068. https://doi.org/10.1115/1.2791905

673 Shahba S, Soltani F (2016) Analysis of stress and displacement of Taham Earth Dam. Indian Journal
674 of Science and Technology 9(45):1-10. https://doi.org/10.17485/ijst/2016/v9i45/104182

675 Souza Junior TF de, Moreira EB, Heineck SK (2018) Mining tailing dams in Brazil. Holos 5:2-39
676 [in Portuguese]. https://doi.org/10.15628/holos.2018.7423

677 Wood DM (2004) Geotechnical Modelling. Taylor e Francis, New York

Figures

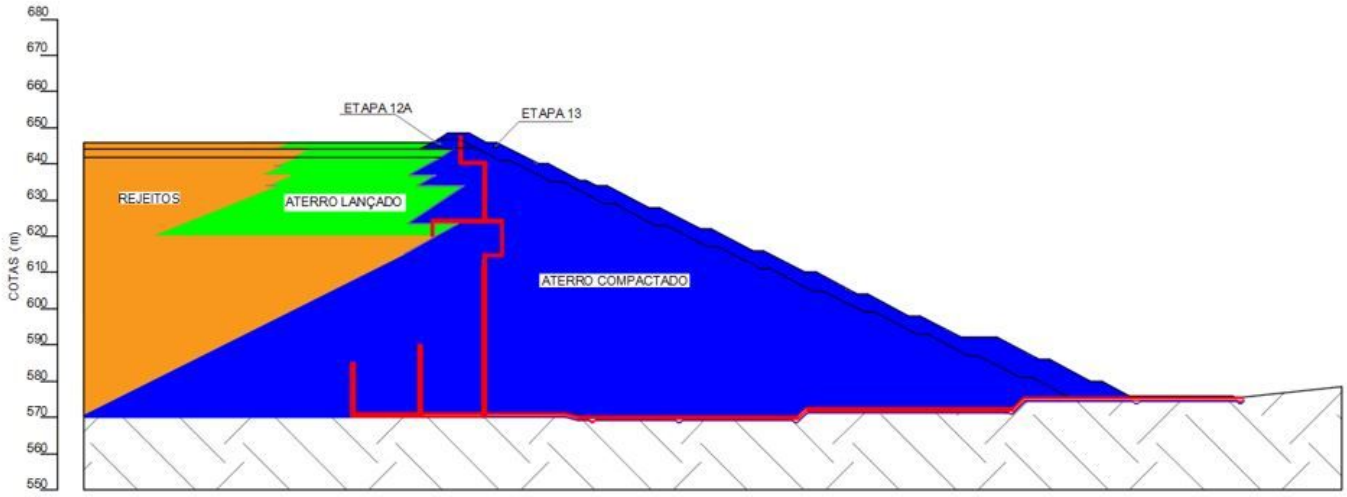

Figure 1

Dam typical section – stages 12A and 13

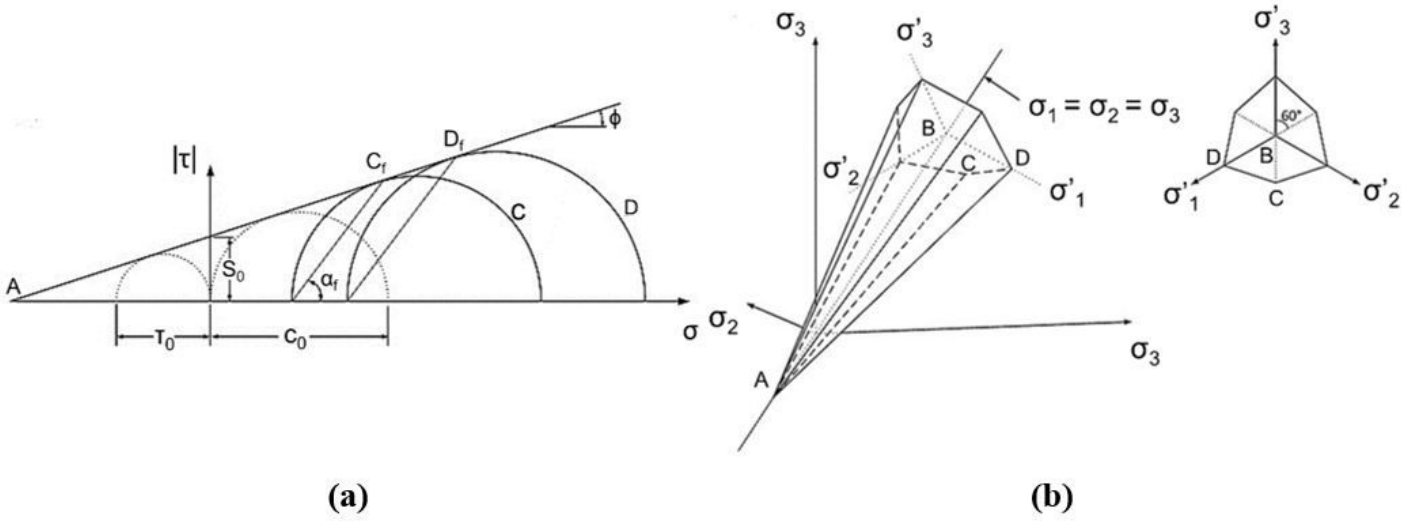

Figure 2

Mohr-Coulomb Criteria: a) Rupture envelope; b) Failure surface. (Source: Labuz and Zang, 2012)

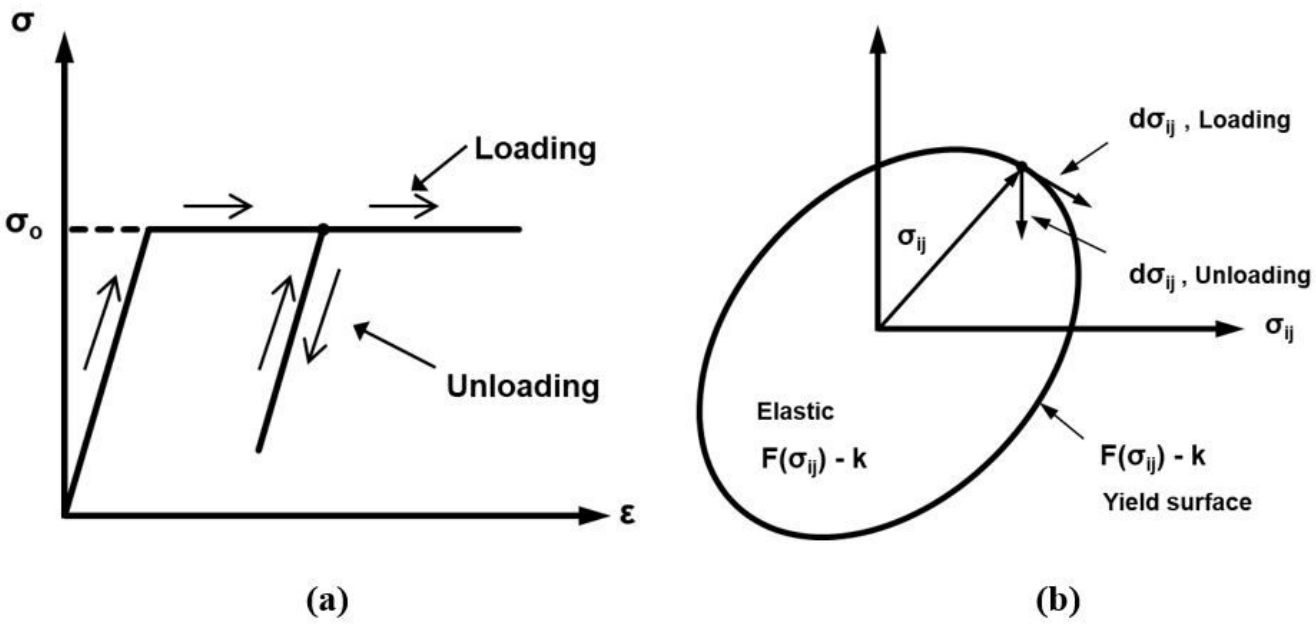

Figure 3

Elastic perfectly plastic model: a) Stress vs deformation behavior; b) Loading and unloading yield surface (Cheb e Han, 1988).

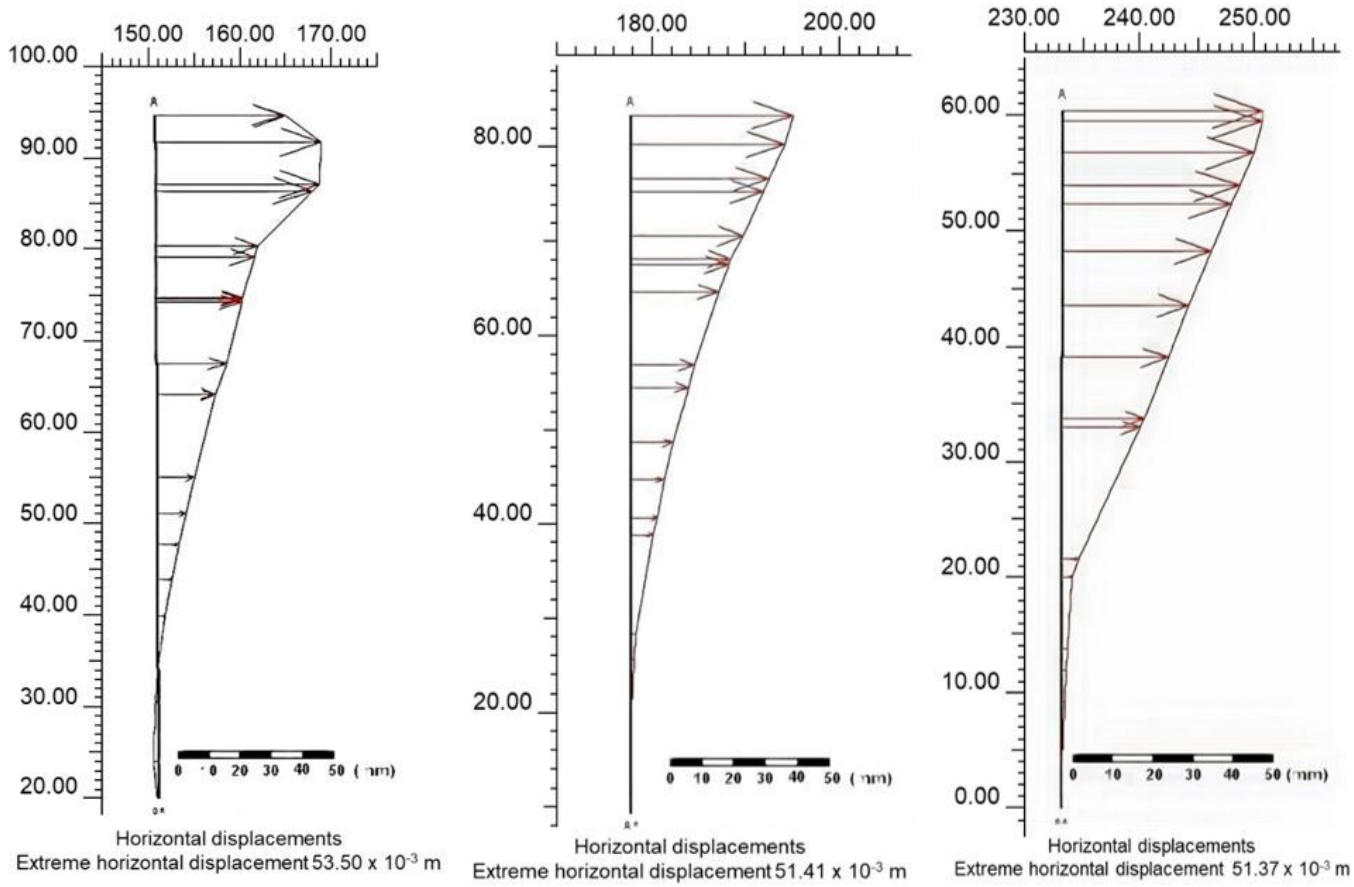

Figure 4

Numerical model horizontal displacements results for the inclinometers (x Direction)

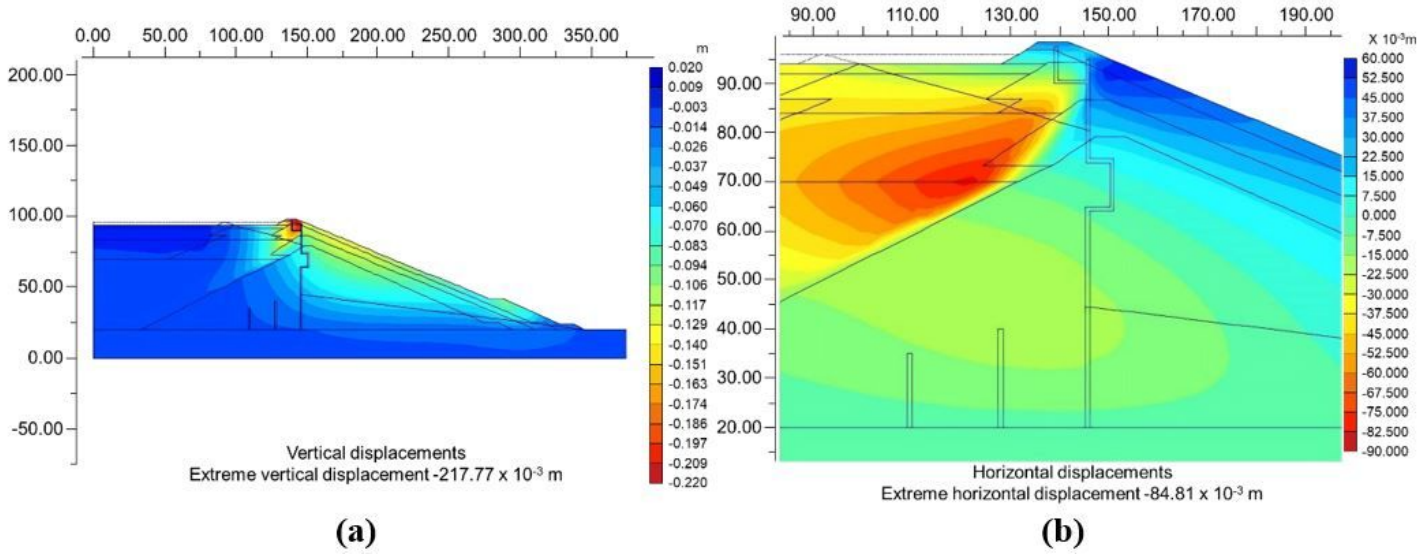

Figure 5

Dam displacements caused by the stage 13 compacted embankment construction: a) vertical (m); b) horizontal (x 10^3 m).

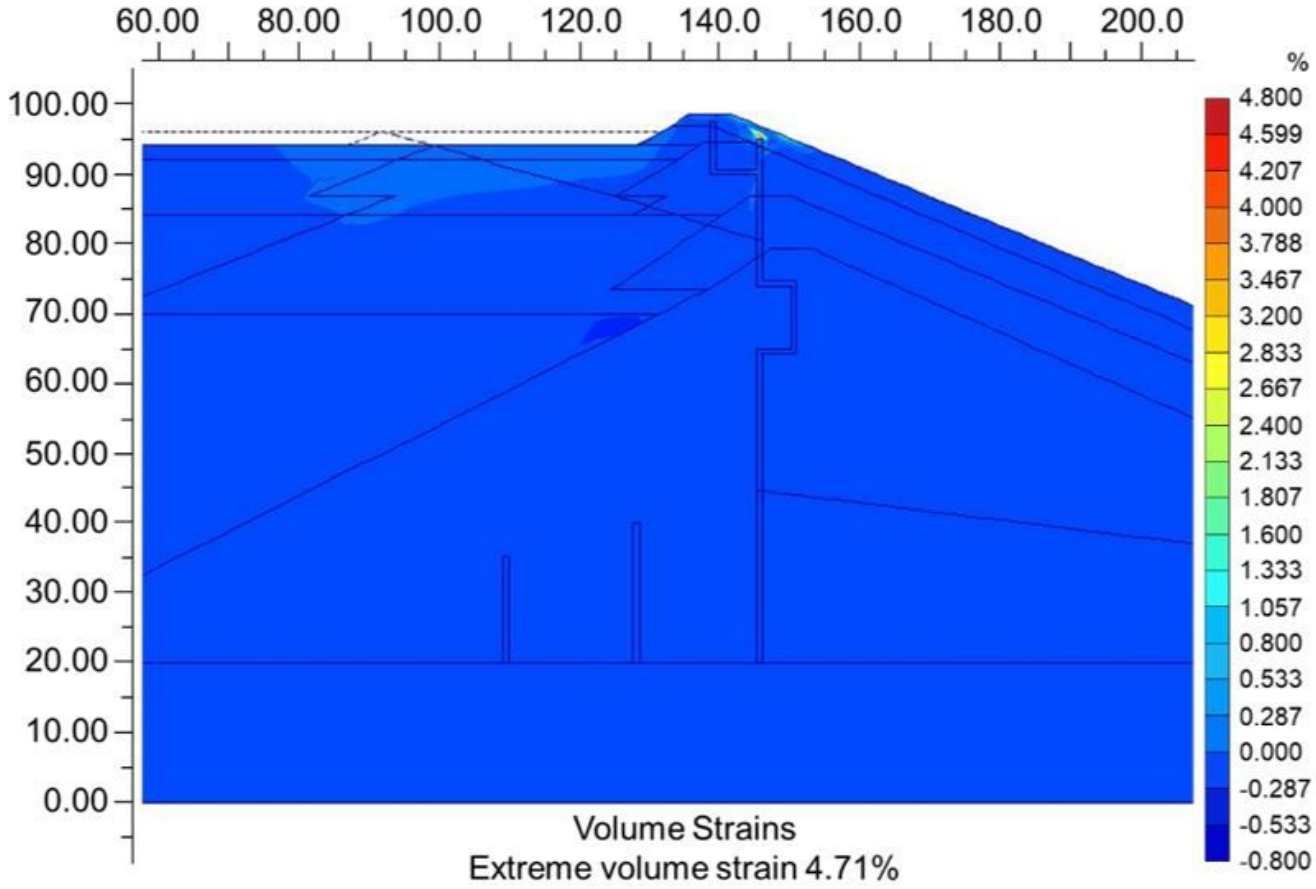

Figure 6

Volumetric deformations on the dam caused by the construction of the compacted embankment of stage 13.

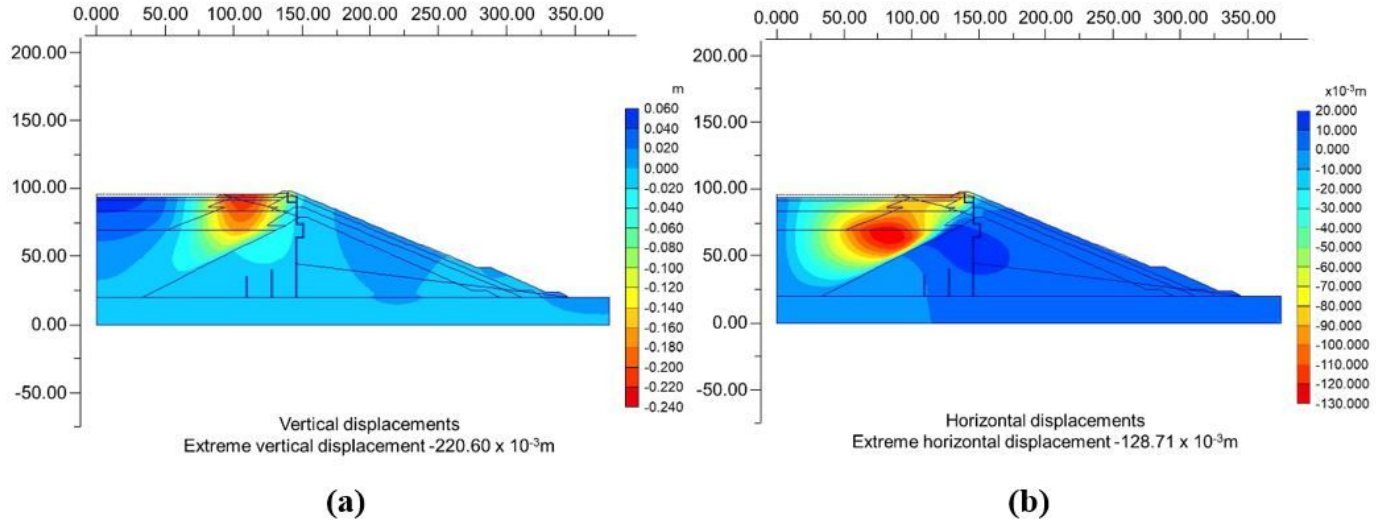

Figure 7

Vertical displacements on the dam, caused by the construction of the stage 13 launched fill: a) Vertical; b) Horizontal

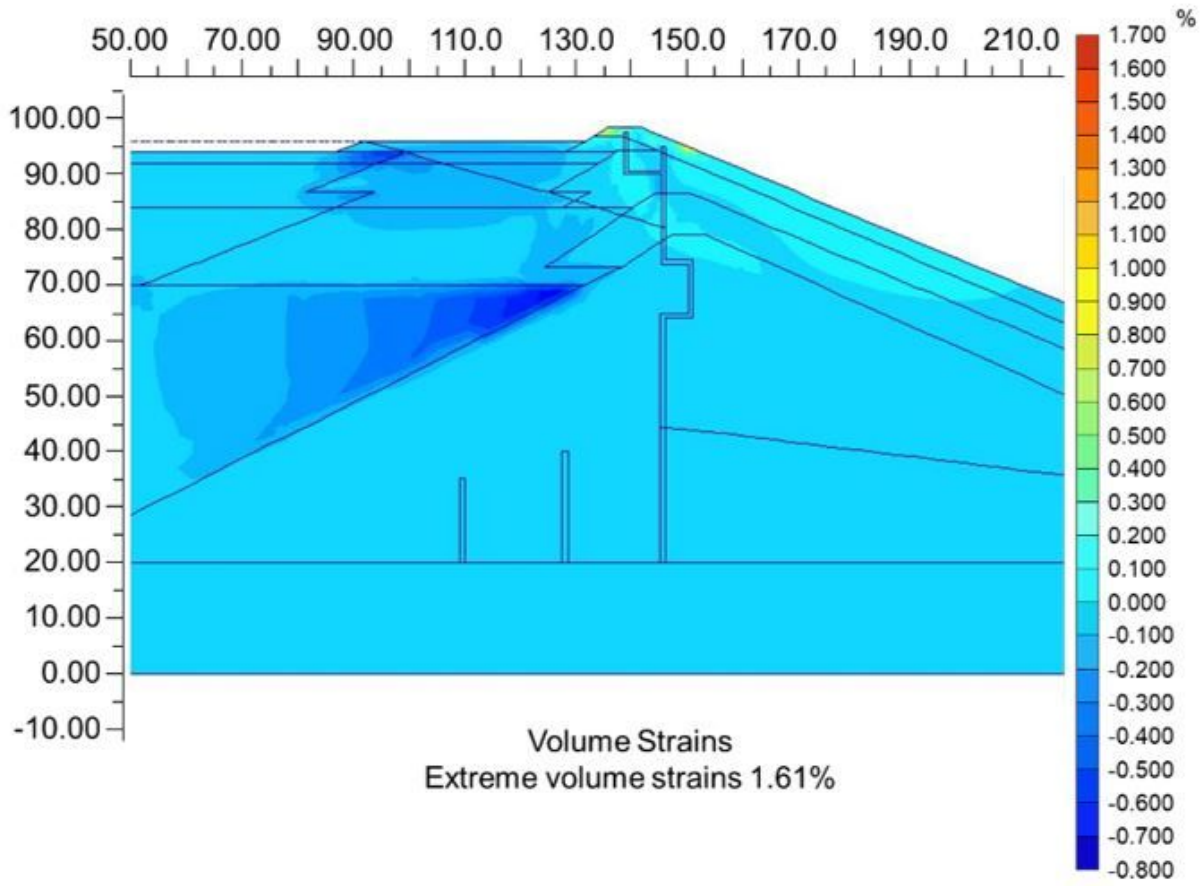

Figure 8

Volumetric deformations on the dam caused by the stage 13 launched landfill construction.

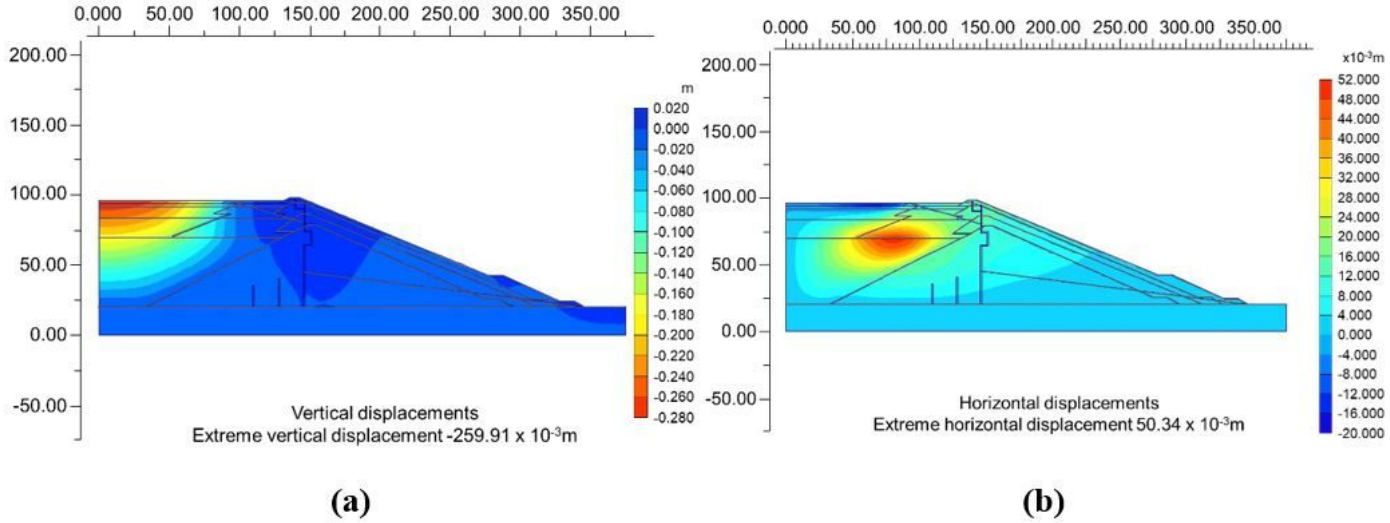

Figure 9

Vertical displacements on the dam originated by the stage 13 reservoir filling: a) Vertical; b) Horizontal

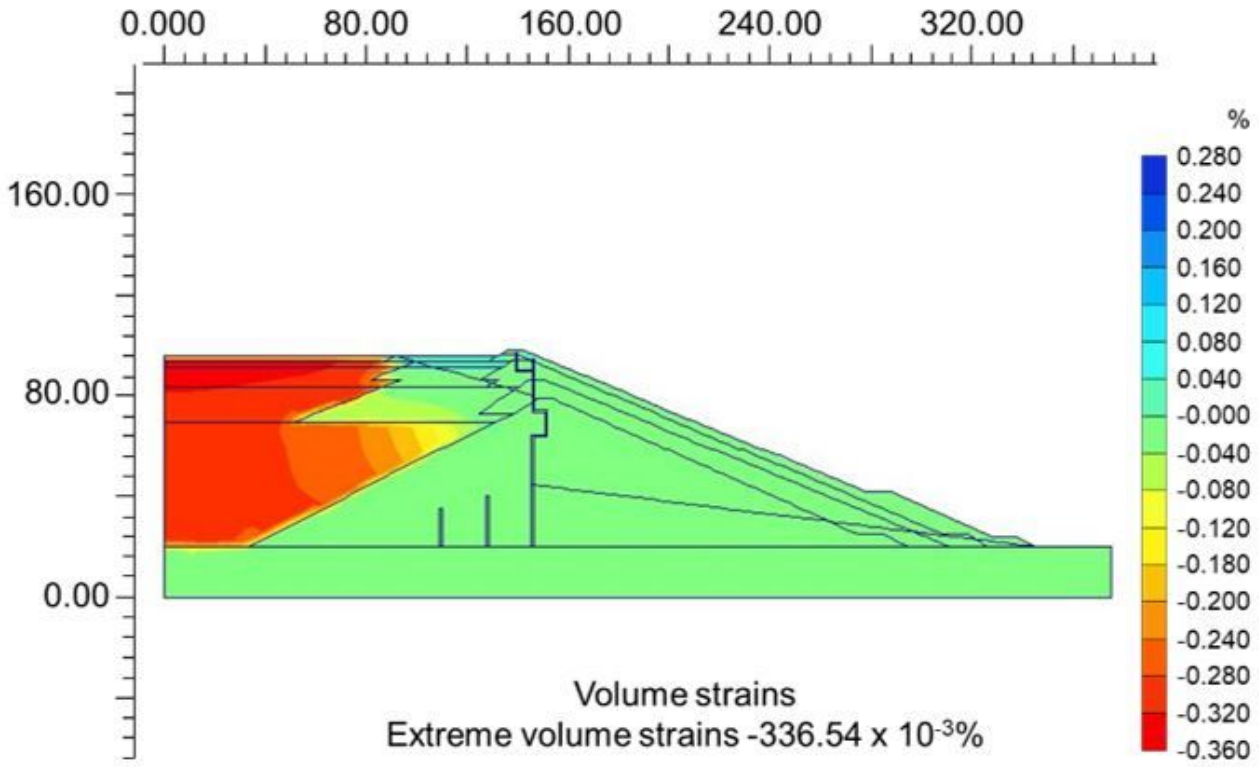

Figure 10

Volumetric deformations on the dam caused by the stage 13 tailings reservoir filling

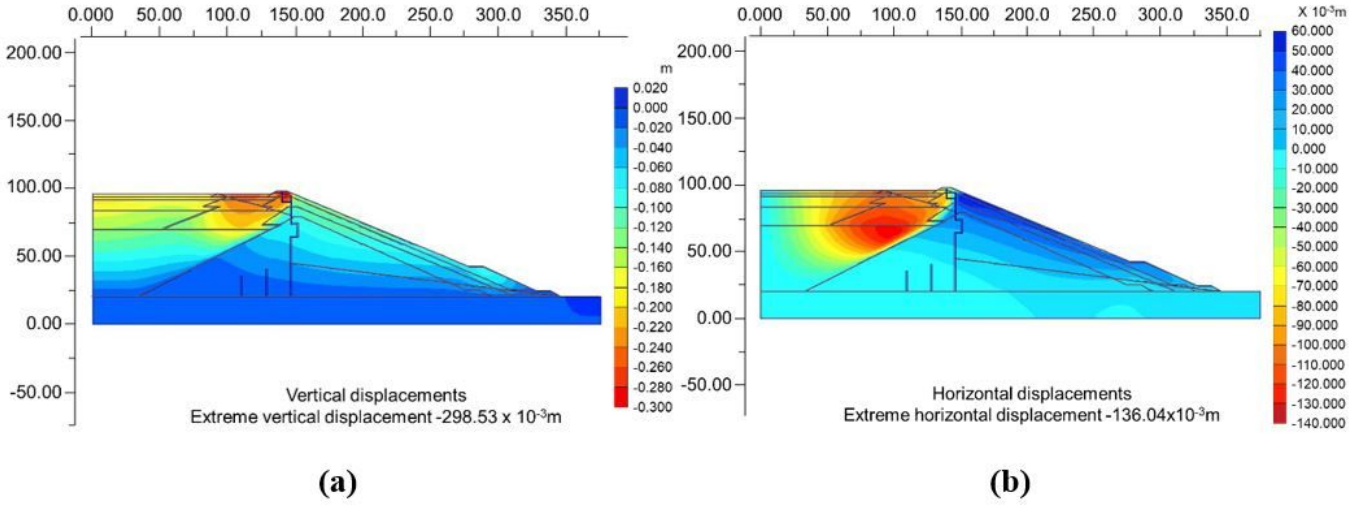

Figure 11

Displacements on the dam due to the stage 13 construction and filling of the reservoir: a) Vertical; b) Horizontal

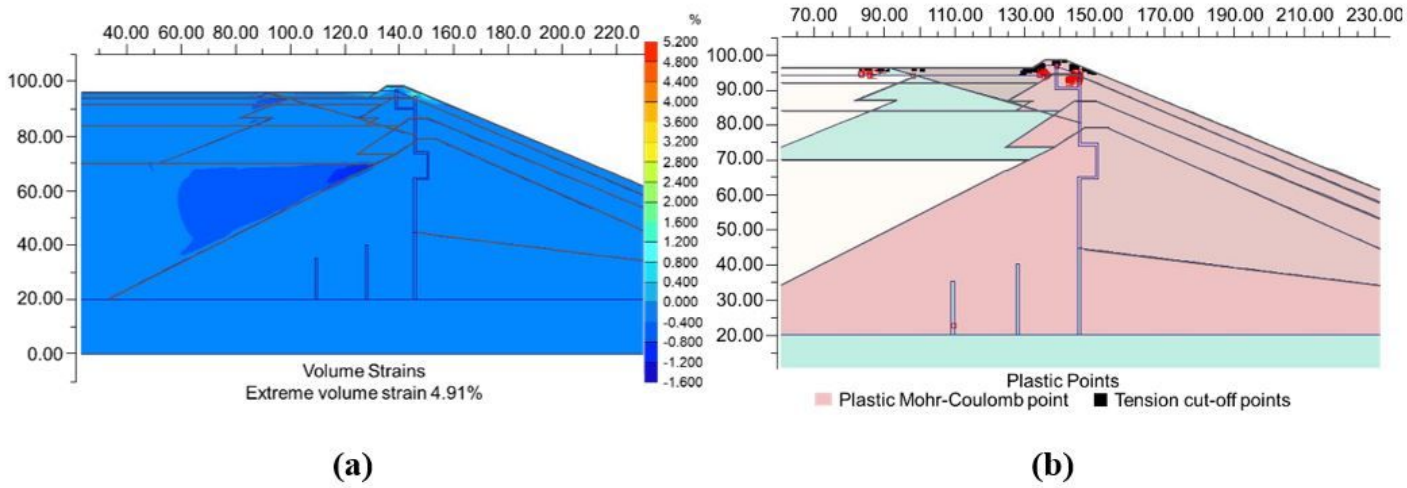

Figure 12

Yield on the dam caused by stage 13 construction and reservoir filling: a) volumetric deformations; b) Evaluation of yield concentration points of the dam

Figure 13

Finite elements of the surface of the model

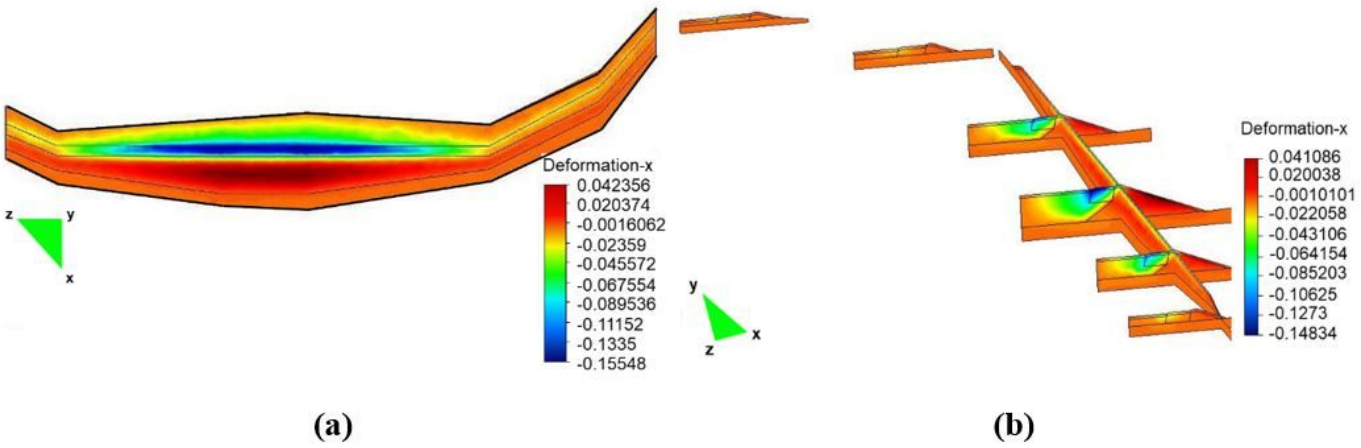

Figure 14

Horizontal displacement on the x direction: a) soil surface; b) massif interior (values in meters)

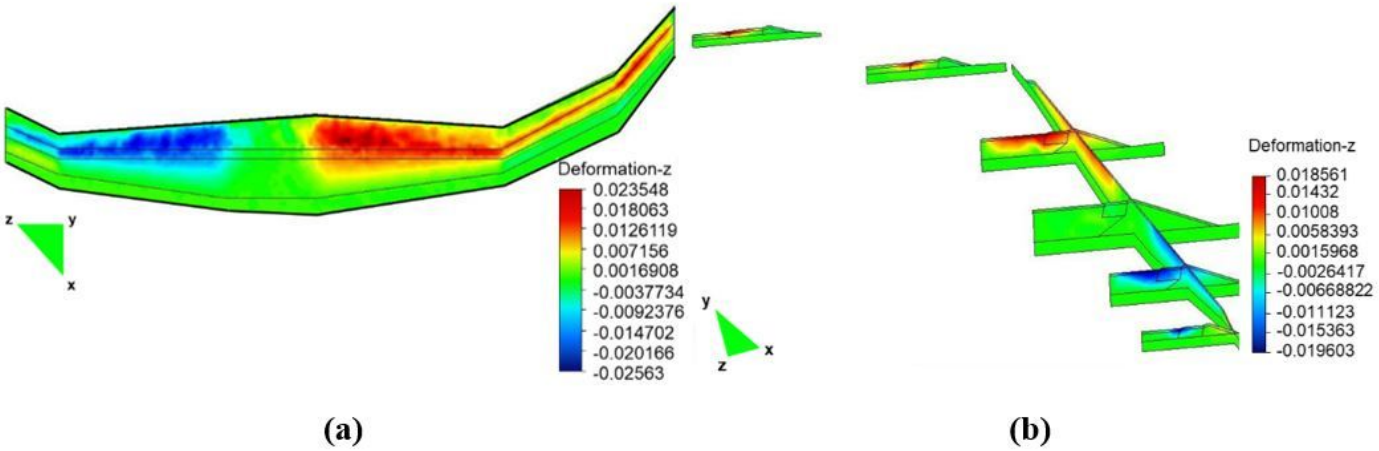

Figure 15

Horizontal displacements on the z direction: a) on the soil surface; b) on the massif interior (values in meters)

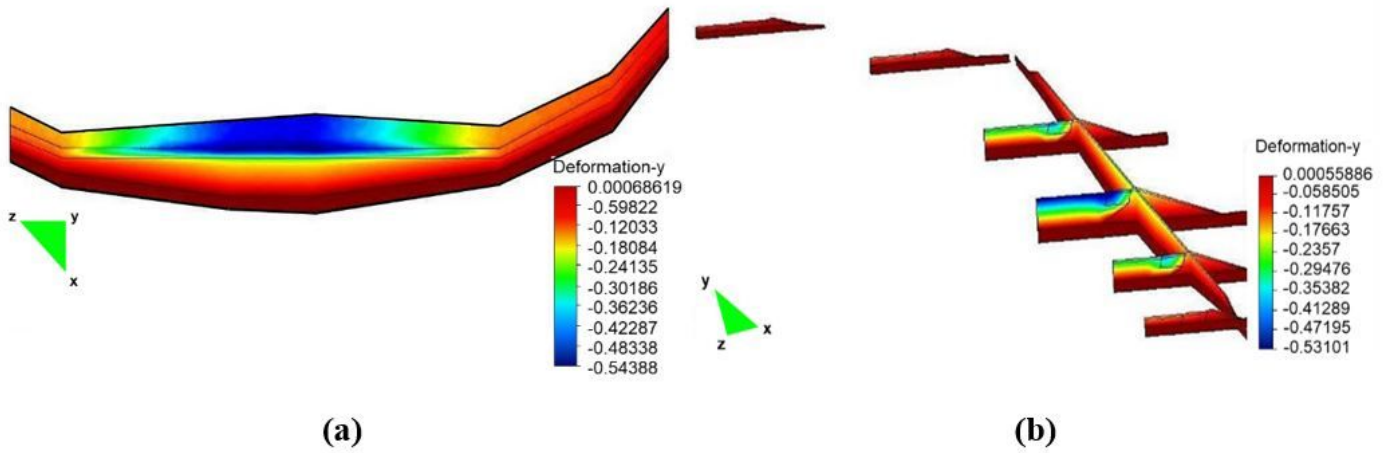

(a) (b)

Figure 16

Vertical displacements on the embankment: a) soil surface; b) in the interior of the massif (values in meters)

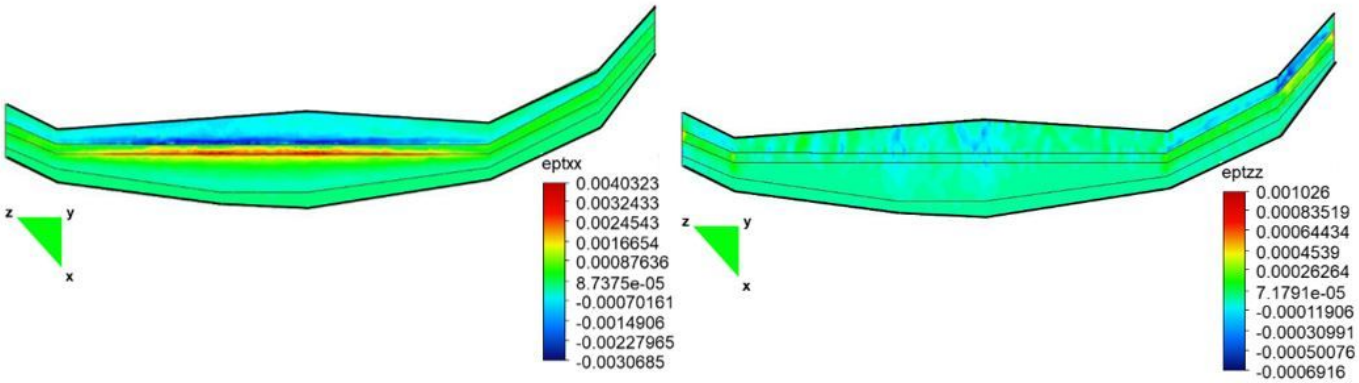

(a) (b)

Figure 17

Total deformations of: a) soil surface on the x direction; b) soil surface on the z direction (values in m/m)

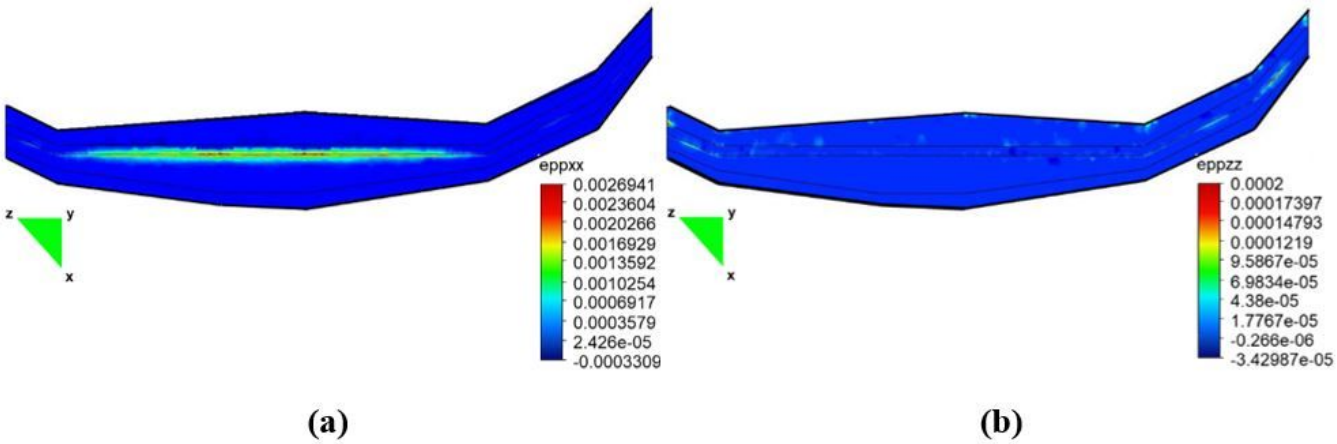

Figure 18

Yield deformations: a) soil surface on the x direction; b) soil surface on the z direction (values in m/m)